FRP COMPOSITES CHARACTERIZATION BY FTIR-IMAGING

A THESIS SUBMITTED IN PARTIAL FULFILMENT
OF THE REQUIREMENT FOR THE DEGREE OF

Bachelor of Technology
in
Metallurgical and Materials Engineering

By

JITENDRA KUMAR BEHERA

Department of Metallurgical and Materials Engineering

National Institute of Technology

Rourkela

2007

FRP COMPOSITES CHARACTERIZATION BY FTIR-IMAGING

A THESIS SUBMITTED IN PARTIAL FULFILMENT
OF THE REQUIREMENT FOR THE DEGREE OF

Bachelor of Technology
in
Metallurgical and Materials Engineering

By

JITENDRA KUMAR BEHERA

Under the Guidance of

Prof. B.C.RAY

Department of Metallurgical and Materials Engineering

National Institute of Technology

Rourkela

2007

National Institute of Technology
Rourkela

CERTIFICATE

This is to certify that the thesis entitle, "*FRP COMPOSITES CHARACTERIZATION BY FTIR-IMAGING*" submitted by **Mr. JITENDRA KUMAR BEHERA** in partial fulfillment of the requirements for the award of Bachelor of Technology Degree in Metallurgical and Materials Engineering at the National Institute of Technology, Rourkela (Deemed University) is an authentic work carried out by him under my supervision and guidance.

To the best of my knowledge, the matter embodied in the thesis has not been submitted to any other University / Institute for the any Degree or Diploma.

Date:

Prof. B.C.RAY
Dept. of Metallurgical and Materials Engineering
National Institute of Technology
Rourkela-769008

ACKNOWLEDGEMENT

I avail this opportunity to extend my hearty indebtedness to my guide **Professor B. C. Ray**, Metallurgical & Materials Engineering Department, for his valuable guidance, constant encouragement and kind help at different stages for the execution of this dissertation work.

I also express my sincere gratitude to **Professor G. S. Agrawal**, Head of the Department, Metallurgical & Materials Engineering, for providing valuable departmental facilities.

I am also grateful to **Mr. Samir Pradhan** and **Mr. Rajesh Pattnaik,** Metallurgical & Materials Engineering Department, for their help in carrying out this work.

I am also grateful to **Ms Neeti Sharma** and **Mr. Surendra Kumar M.** for their help in understanding the various things related to my project.

Last but not least I thank technical assistants of metallurgical Dept. and my friends to help me directly or indirectly to complete this project successfully.

JITENDRA KUMAR BEHERA
B.Tech
Metallurgical and Materials Engineering

Contents

ABSTRACT

It is well known that the high-performance properties of glass-fiber-reinforced polymer composite materials are not simply the sum of the properties of their constituents. The properties of composites depend on the ability of the interface to transfer stress from the matrix to the reinforcement. In fact, it is at the interfacial region where stress concentrations develop because of differences in the thermal expansion coefficients between the reinforcement and the matrix phase due to loads applied to the structure, cure shrinkage (in thermosetting matrices), and crystallization (in some thermoplastic matrices). Coupling agents have two different functionalities that are designed to chemically bond with the reinforcement at one end and the organic matrix at the other. The most commonly used coupling agents are bifunctional organosilicon compounds named silanes. The silane coupling agents of most commercial glass fibers have three hydrolyzable alkoxy functional groups. These groups allow the silanes to react with each other and with the glass to form a multilayer network on the glass surface.

In order to study the effect of moisture absorption by the glass-fiber surface to the bulk epoxy, we used FTIR imaging to investigate this problem. Furthermore, to the best of our knowledge, there are no studies of the epoxy/glass fiber interface using the “FTIR imaging” technique. This technique uses a focal-plane array detector (FPA) coupled with a step scan interferometer to improve FTIR microscopic measurements, yielding spatially resolved spectroscopic information in the infrared region. In addition, this technique allows one to obtain consecutive IR images of the microscopic region of interest in intervals of time less than 5 min. For this reason, the FTIR imaging can be used to study the evolution of several components at the same time in specific sites in the sample. The composite was fabricated using the conventional HAND LAYOUT method. The materials used are E-Glass Fiber and Epoxy resin (araldite LY556). The hardener used is HY951. A sixteen layered structure was formed as per the ASTM standards. The fiber and the matrix were taken in the ratio of 50:50. The sample was left for drying for 24 Hrs after the fabrication so that the matrix completely seeps in and become dry. The samples after cutting and oven drying were divided into 3 parts. One part is kept as such and was wrapped in Aluminium foil and stored in the Dessicator after weighing all the samples. Second and third part were first weighed and then given a hygrothermal treatment by placing the samples in the humidity chamber for 50 Hrs and 100 Hrs respectively at 50°C and 95% humidity. After

the Hygrothermal treatment, the dimensions of all the samples were measured and then they were being tested for 3-Point Bend Test. Then the samples were characterized using FTIR-Imaging and he fractured surface was studied by SEM. The ILSS value increases with initial moisture absorption due to the relief of residual stresses but after a certain stage it decreases due to the loss of adhesion between matrix and fiber. The ILSS value increases with the strain rate but after a certain stage it decreases because the matrix is unable to transfer load properly i.e. ILSS value is low at low strain rate as well as high strain rate as at low strain the load is applied for more time and thus the specimen fails at low stress value and at high strain rate, the time available for transfer of load is insufficient and the load acts as an impact and thus specimen fails at low stress. Thus the rate of loading should be optimum. The FTIR-IMAGING Results Shows that the moisture absorption is more at the interface in low Hrs treatment as the components of composites have the property to absorb moisture and then moisture absorption is more in matrix due to more debonding leading to creation of voids at the interface and thus the water diffuses in easily through the interface to matrix. The SEM Images of the fractured surfaces shows that the initial moisture absorption results in the increase in the bond strength as the matrix gets squeezed but after a saturation stage, the moisture absorption results in the debonding of the matrix-interface bond and also matrix-matrix bond and thus ILSS value initially increases and then decreases.

CHAPTER 1

INTRODUCTION

1. INTRODUCTION

It is well known that the high-performance properties of glass-fiber-reinforced polymer composite materials are not simply the sum of the properties of their constituents. The final performance of a fiber-reinforced composite depends on the fiber properties and architecture, the extent of resin cure and resultant matrix properties, the quality of the mold filling, and the nature of the fiber/polymer matrix interface (the region between the fiber and the matrix). The properties of composite materials are strongly influenced by the type of adhesion between the reinforcement and the matrix. In many cases failure occurs in the interface region due to chemical reactions or plasticizing when impurities (commonly water) penetrate the interface. The properties of composites depend on the ability of the interface to transfer stress from the matrix to the reinforcement. In fact, it is at the interfacial region where stress concentrations develop because of differences in the thermal expansion coefficients between the reinforcement and the matrix phase due to loads applied to the structure, cure shrinkage (in thermosetting matrices), and crystallization (in some thermoplastic matrices).

The important effects of the interface on the properties of glass-fiber-reinforced composites have led to considerable efforts to understand, control, and specifically modify it. Surface treatments of fiber and particle reinforcements are common methods to improve the general adhesion properties by increasing electrostatic interactions and/or facilitating chemical bonding between the constituents. Coupling agents have an effect on the interface structure and properties. Coupling agents have two different functionalities that are designed to chemically bond with the reinforcement at one end and the organic matrix at the other. The most commonly used coupling agents are bifunctional organosilicon compounds named silanes. The silane coupling agents of most commercial glass fibers have three hydrolyzable alkoxy functional groups. These groups allow the silanes to react with each other and with the glass to form a multilayer network on the glass surface. These are used to treat glass fibers to promote adhesion and covalent bonding between the fibers and the polymeric matrix. It was reported that the silane coupling agents deposit on the glass surface as three fractional layers, with the molecules connected through siloxane bonds. Three types of bonding between the coupling agent and matrix resin have been reported: chemical bondmg, hydrogen bondmg, and interpenetrating polymer network. The performance of polymeric composites is a function of the interfacial properties. The chemical bonds formed between the fiberglass and polymeric resin, through the use of a silane coupllng agent, improves the mechanical strength of composites. Most sigmficantly, the wet strength is

improved under moist conditions and the dry strength properties return after dehydration. Apparently, the hydrolysis of some bonds in the silane/glass interphase is a reversible process. Hydrolytic attack on glass-reinforced plastic composites has been studied extensively by FTIR spectroscopy over the past ten years. However, this technique has yielded only a FTIR spectrum that is a combination of the bulk and interphase of the composites. Since the development of FTIR micro spectroscopy, detailed analyses of the spatial distribution of chemical species in the composite have been obtained. This is achieved by utilizing a spatial resolution of ten micrometers.

In order to study the effect of moisture absorption by the glass-fiber surface to the bulk epoxy, we used FTIR imaging to investigate this problem. Furthermore, to the best of our knowledge, there are no studies of the epoxy/glass fiber interface using the "FTIR imaging" technique. This technique uses a focal-plane array detector (FPA) coupled with a stepscan interferometer to improve FTIR microscopic measurements, yielding spatially resolved spectroscopic information in the infrared region. In addition, this technique allows one to obtain consecutive IR images of the microscopic region of interest in intervals of time less than 5 min. For this reason, the FTIR imaging can be used to study the evolution of several components at the same time in specific sites in the sample. The multicomponent detection capability and good temporal resolution were demonstrated in studies of polymer dissolution, polymer curing, and diffusion processes. In this work it is proposed to study the effect of moisture absorption on an epoxy system at the interface formed with a glass fiber and also in the bulk of the matrix.

CHAPTER 2

LITERATURE SURVEY

2. LITERATURE SURVEY

2.1. Composites

A composite is combination of two materials in which one of the materials, called the reinforcing phase, is in the form of fibers, sheets, or particles, and is embedded in the other materials called the matrix phase. The reinforcing material and the matrix material can be metal, ceramic, or polymer. Composites are used because overall properties of the composites are superior to those of the individual components. For example: polymer/ceramic composites have a greater modulus than the polymer component, but aren't as brittle as ceramics. The following are some of the reasons why composites are selected for certain applications:

- High strength to weight ratio (low density high tensile strength)
- High creep resistance
- High tensile strength at elevated temperatures
- High toughness

Three types of composites are:

- Particle-reinforced composites
- Fiber-reinforced composites
- Structural composites

2.2. Fiber-Reinforced Composites:

Reinforcing fibers can be made of metals, ceramics, glasses, or polymers that have been turned into graphite and known as carbon fibers. Fibers increase the modulus of the matrix material. The strong covalent bond along the fiber's length gives them a very high modulus in this direction because to break or extend the fiber the bonds must also be broken or moved. Fibers are difficult to process into composites which makes fiber-reinforced composites relatively expensive. Fiber-reinforced composites are used in some of the most advanced, and therefore most expensive, sports equipment, such as a time-trial racing bicycle frame which consists of carbon fibers in a thermoset polymer matrix. Body parts of race cars and some automobiles are composites made of glass fibers (or fiberglass) in a thermoset matrix.

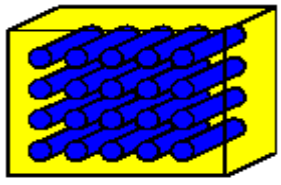

Fig 2.1. Schematic diagram of FRP Composite

INFLUENCE OF FIBER LENGTH:

The mechanical characteristics of a fiber reinforced composites depend not only on the properties of the fiber, but also on the degree to which an applied load is transmitted to the fibers by the matrix phase. Important to the extent of this load transmittance is the magnitude of the interfacial bond between the fiber and matrix phases. Some critical fiber length is necessary for effective strengthening and stiffening of the composite material. This critical length l_c is dependent on the fiber diameter d and its ultimate (or tensile) strength σ_f^*, and on the fiber matrix bond strength (or shear yield strength of the matrix, whichever is smaller) τ_c according to

$l_c = \sigma_f^* / 2\,\tau_c$

for a number of glass and carbon fiber –matrix combinations, this critical length is of the order of 1mm, which ranges between 20 and 150 times the fiber diameter. When a stress equal to σ_f^* is applied to a fiber having just this critical length maximum fiber load is achieved only at the axial center of the fiber. Fibers for which $l >> l_c$ (normally $l > 15 l_c$) are termed continuous; discontinuous or short fibers have lengths shorter than this. For discontinuous fibers lengths significantly less than l_c, the matrix deforms around the fiber such that there is virtually no stress transference and little reinforcement by the fiber. To affect a significant improvement in strength of the composite, the fibers must be continuous.

INFLUENCE OF FIBER ORIENTATION:

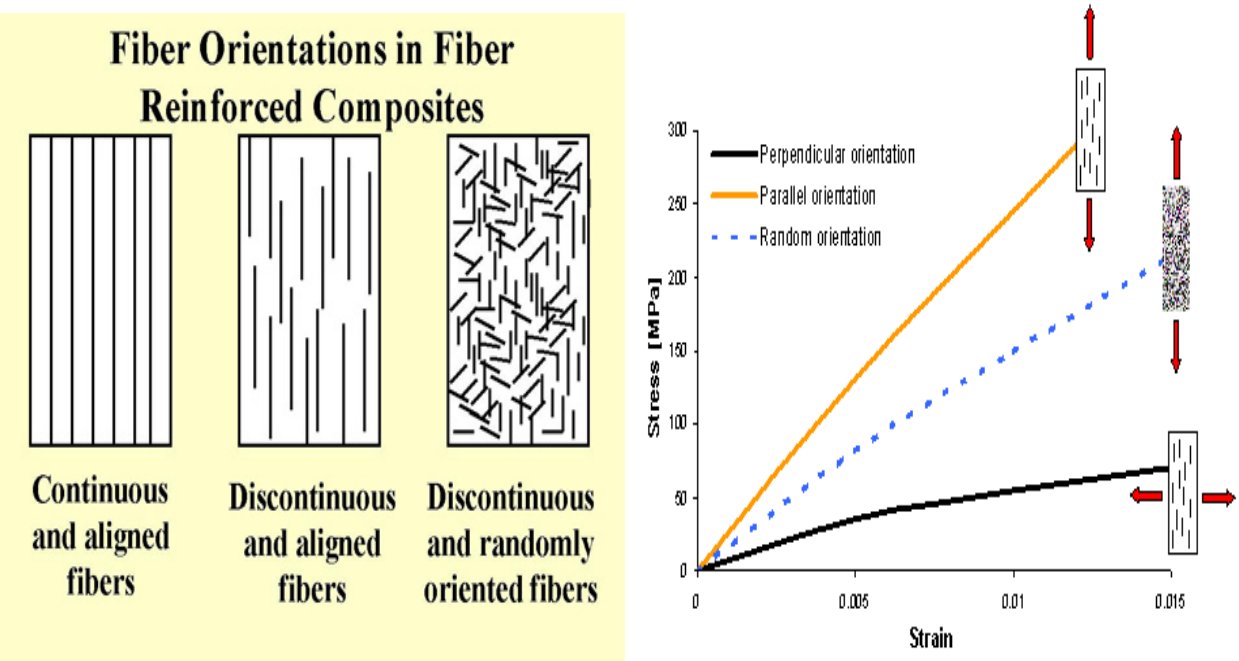

Fig 2.2. Effect of Fiber Orientation on the strength of FRP Composites

MODULUS OF FIBER-REINFORCED COMPOSITES:

Fibers have a very high modulus along their axis, but have a low modulus perpendicular to their axis. If the fibers are all parallel, the modulus of a fiber reinforced composite depends upon which direction you're measuring. The modulus of the entire composite, matrix plus reinforcer, is governed by the rule of mixtures when measuring along the length of the fiber:

$E_c = E_f V_f + E_m V_m$

E_c is the modulus of the entire composite along the length of the fiber.

E_f is the modulus of the fiber along the length of the fiber.

V_f is the volume percent occupied by the fibers.

E_m is the modulus of the matrix (usually not dependent upon direction)

V_m is the volume percent occupied by the matrix (equal to (1-Vf)).

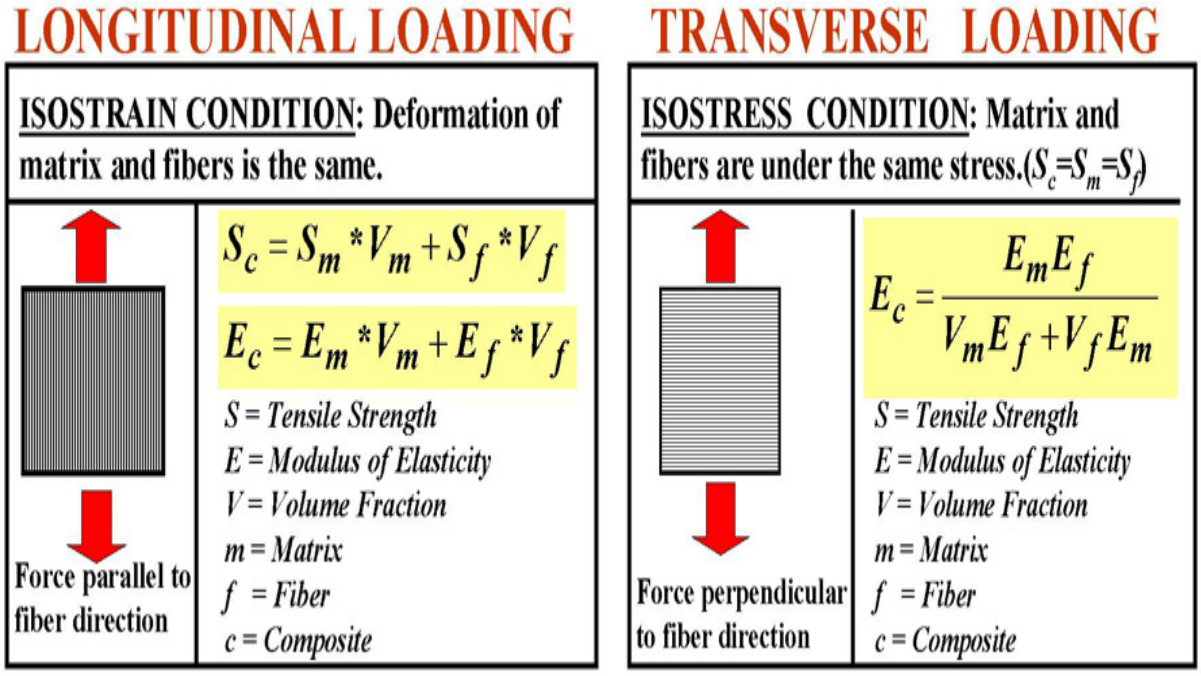

Fig 2.3. Comparison of Loading type on Strength and Modulus of Elasticity

2.2.1. Types of Fibers Used in Fiber Reinforced Composites:

1. Glass fibers
2. Carbon fibers
3. Aramid fibers

Glass Fibers

The most common reinforcement for the polymer matrix composites is a glass fiber. Most of the fibers are based on silica (SiO_2), with addition of oxides of Ca, B, Na, Fe, and Al. The glass fibers are divided into three classes -- E-glass, S-glass and C-glass. The E-glass is designated for electrical use and the S-glass for high strength. The C-glass is for high corrosion resistance, and it is uncommon for civil engineering application. Of the three fibers, the E-glass is the most common reinforcement material used in civil structures. It is produced from lime-alumina-borosilicate which can be easily obtained from abundance of raw materials like sand. The glass fiber strength and modulus can degrade with increasing temperature. The fiber itself is regarded as an isotropic material and has a lower thermal expansion coefficient than that of steel.

1. *E-glass (electrical)*

Family of glassed with a calcium aluminum borosilicate composition and a maximum alkali composition of 2%. These are used when strength and high electrical resistivity are required.

2. *S-glass (tensile strength)*

Fibers have a magnesium aluminosilicate composition, which demonstrates high strength and used in application where very high tensile strength required.

3. *C-glass (chemical)*

It has a soda lime borosilicate composition that is used for its chemical stability in corrosive environment. It is often used on composites that contain or contact acidic materials.

Constituent	Weight percentage
SiO2	54
Al203	14
CaO+MgO	12
B2O3	10
Na2O+K2O	Less than 2
Impurities	Traces

Table 2.1. Composition of E-Glass

Typical Properties	**E-Glass**	**S-Glass**
Density (g/cm^3)	2.60	2.50
Young's Modulus (GPa)	72	87
Tensile Strength (GPa)	1.72	2.53
Tensile Elongation (%)	2.4	2.9

Table2.2 Comparison of Properties of Glass Fiber

Carbon Fibers:

Carbon fiber is the most expensive of the more common reinforcements, but in space applications the combination of excellent performance characteristics coupled with light weight make it indispensable reinforcement with cost being of secondary importance Carbon fibers consist of small crystallite of turbostratic graphite. These resemble graphite single crystals except that the layer planes are not packed in a regular fashion along the c-axis direction. In a graphite single crystal the carbon atoms in a basal plane are arranged in hexagonal arrays and held together by strong covalent bonds. Between the basal planes only weak Vander-waal forces exist. Therefore the single crystals are highly anisotropic with the plane moduli of the order of 100 GPa whereas the molecules perpendicular to the basal plane are only about 75 GPa. It is thus evident that to produce high modulus and high strength fibers, the basal planes of the graphite must be parallel to the fiber axis. They have lower thermal expansion coefficients than both the glass and aramid fibers. The carbon fiber is an anisotropic material, and its transverse modulus is an order of magnitude less than its longitudinal modulus. The material has a very high fatigue and creep resistance. Since its tensile strength decreases with increasing modulus, its strain at rupture will also be much lower. Because of the material brittleness at higher modulus, it becomes critical in joint and connection details, which can have high stress concentrations. As a result of this phenomenon, carbon composite laminates are more effective with adhesive bonding that eliminates mechanical fasteners.

The basic unit of PAN is:

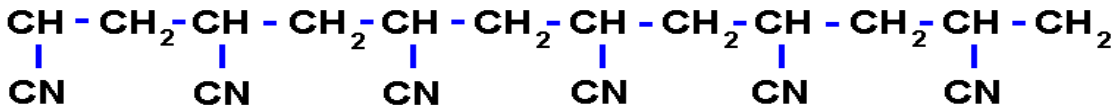

The conversion of PAN to carbon fibers is done as shown under:-

- *OXIDATION* involves heating the fibers to around 300 ºC in air. This evolves hydrogen from the fibers and adds less volatile oxygen**.**

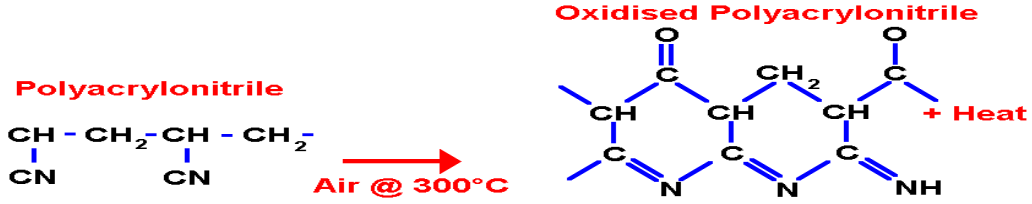

- *CARBONISATION (GRAPHITISATION)* involves heating the fibers up to 3000 °C in an inert atmosphere; the fibers are now nearly 100 % carbon.

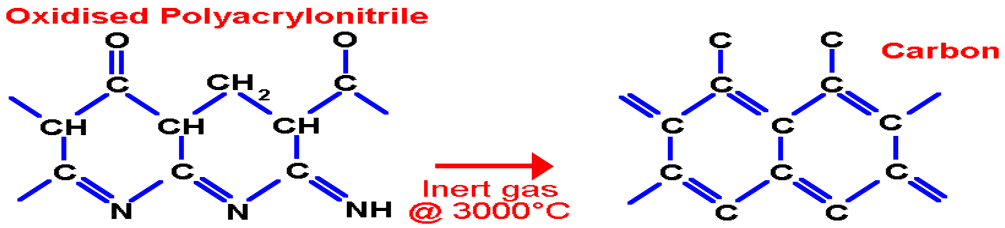

The temperature will determine the *grade* of fiber produced:

Grades *of Carbon Fiber*				
Carbonization Temperature (°C)	to 1000	1000 - 1500	1500 - 2000	2000 + (Graphitization)
Grade of Carbon Fiber	**Low Modulus**	**Standard Modulus**	**Intermediate Modulus**	**High Modulus**
Modulus of Elasticity (GPa)	to 200	200 - 250	250 - 325	325 +

Table 2.3. Grades of Carbon Fiber

Carbon fibers are derived from one of two precursor materials

- *PITCH*
- *PAN (Polyacrylonitrile fibers)*

PITCH based carbon fibers have lower mechanical properties and are therefore rarely used in critical structural applications. *PAN* based carbon fibers are under continual development and are used in composites to make materials of great strength and lightness.

Typical Properties	**Density (g/cm^3)**	**Young's Modulus (GPa)**	**Tensile Strength (GPa)**	**Tensile Elongation (%)**
High Strength	1.8	230	2.48	1.1
High Modulus	1.9	370	1.79	0.5
Ultra-High Modulus	2.0 - 2.1	520 - 620	1.03 - 1.31	0.2

Table 2.4.Comparison of properties of carbon fibers.

2.2.2. Epoxy Resin

Epoxy or **polyepoxide** is a thermosetting epoxide polymer that cures (polymerizes and crosslinks) when mixed with a catalyzing agent or "hardener". Most common epoxy resins are produced from a reaction between epichlorohydrin and bisphenol-A. The applications for epoxy based materials are extensive and include coatings, adhesives and composite materials such as those using carbon fiber and fiberglass reinforcements, (although polyester, vinyl ester, and other thermosetting resins are also used for glass-reinforced plastic). The chemistry of epoxies and the range of commercially available variations allows cure polymers to be produced with a very broad range of properties. In general, epoxies are known for their excellent adhesion, chemical and heat resistance, good to excellent mechanical properties and very good electrical insulating properties, but almost any property can be modified (for example silver-filled epoxies with good electrical conductivity are widely available even though epoxies are typically electrically insulating).

2.2.3. Advantages of Composites over Metals

1. Fewer components involved because complex shapes can be manufactured in single molding operations.
2. Freedom of shape because of the manufacture processes available.
3. Inexpensive prototypes because trial fabrication can be done with cheap machine tools.

2.3. Hygrothermal Diffusion

Hygrothermal Diffusion usually takes place in presence of thermal and moisture gradients. In many cases water absorption obeys Fick's Law and diffusion is driven by the moisture concentration gradient between the environment and material producing continuous absorption until saturation is reached. The atoms migrate from region of higher concentration to that of lower concentration. The rate of diffusion increases rapidly with the rise in temperature. The concentration gradient of moisture is developed due to the non-uniform distribution of moisture. The presence of imperfections and internal stresses also accelerates the process of diffusion. Epoxy resin absorbs water from the atmosphere from the surface layer reaching equilibrium with the surrounding environment very quickly followed by diffusion of water into all the material. The water absorbed is not usually in liquid form but consists of molecules or group of molecules

linked by hydrogen bonds to the polymer. In addition water can be absorbed by capillary action along any crack which may be present or along the fiber-matrix interface.

The Fickian diffusion process is influenced mainly by two factors:

(a) The internal (fiber volume fraction and its orientation)

(b) The external (relative humidity and temperature).

2.3.1. Theory of Moisture Absorption:

Percentage weight gain was determined as:

$$M = \frac{\text{(Weight of specimen – Weight of dry specimen)}}{\text{(Weight of dry specimen)}} \times 100$$

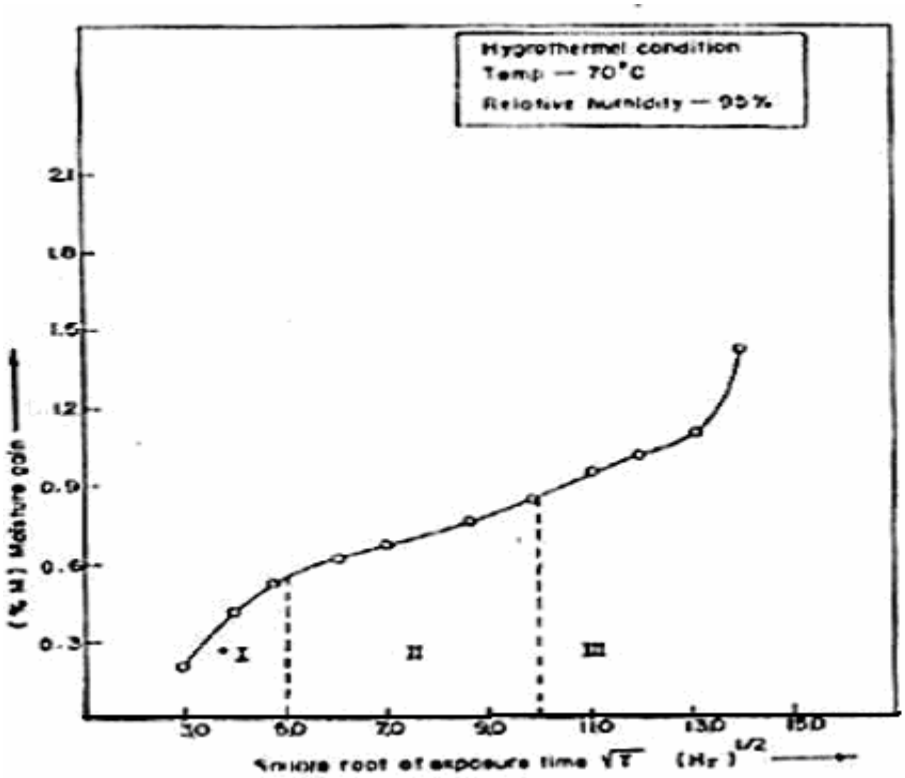

Fig 2.4 Moisture absorption Kinetics

Description of the different stages in moisture absorption kinetics:

- **Stage 1**: Moisture absorption is Fickian.
- **Stage 2:** There is a deviation from linearity with the time axis (reaching saturation, so decrease in slope).

- **Stage 3:** Total non-Fickian pattern (there is a development of micro cracks which enable rapid moisture diffusion, so rapid increase in percentage of moisture).

Non-Fickian behavior:

Fickian behavior is observed in the rubbery state of polymers but often fails to diffusion behavior in glassy polymers. The deviation from Fickian behavior occurs when:-

(a) Cracks or delamination develops.
(b) Moisture diffusion takes place along the fiber matrix interface.
(c) Presence of voids in the matrix.

The nature of diffusion behavior whether Fickian or non Fickian depends on the relative rate at which the polymer structure and the moisture distributions change. When the diffusion rates are much slower than the rate of relaxation, the diffusion has to be Fickian. Non Fickian behavior pertains to the situations when the relaxation processes progress at a rate comparable to the diffusion process. Hygrothermal diffusion in polymeric composites is mostly Fickian type, but non-Fickian behavior is also common for glass/epoxy composite. Absorbed moisture in the composite certainly deteriorates the matrix dominated properties but he effect is more pronounced at higher temperatures and at lower strain rates. The ILSS values are the worst affected property due to this moisture absorption.

2.3.2. Effect of moisture absorption on FRP's properties:

It is now well known that the exposure of polymeric composites in moist environments, under both normal and sub-zero conditions, leads to certain degradation of its mechanical properties which necessitates proper understanding of the correlation between the moist environment and the structural integrity. It is well known that there is a degradation of material property during its service life, as it is often subjected to environments with high temperature and humidity or having a sharp rise and fall of temperature (thermal spikes The absorption of moisture can be attributed largely to the affinity for moisture of specific functional groups of a highly polar nature in the cured resin. The absorption of moisture causes plasticization of the resin to occur with a concurrent swelling and lowering the glass transition temperature of the resin. This adversely affects the fiber-matrix adhesion properties, resulting debonding at fiber/matrix interfaces, micro-cracking in the matrix, fiber fragmentations, continuous cracks and several other phenomena that actually degrades the mechanical property of the composites.

2.4. 3-Point Bend Test

The FRP is subjected to three – point bending until the layers delaminates. When this occurs, the stiffness of the specimen as a whole decreases, which translates as a drop in load in the load - displacement curve? The three-point bend fixture should include two 5 mm diameter supports forming a 36 mm span and a 10 mm diameter load application roller set in the middle of he span. The crosshead speed is 0.5 mm/min unless otherwise specified. Test should be performed at 23 ± 2 °C.The three point bending flexural test provides values for the modulus of elasticity in bending E_B, flexural stress σ_f, flexural strain ε_f and the flexural stress-strain response of the material. The main advantage of a three point flexural test is the ease of the specimen preparation and testing. However, this method has also some disadvantages: the results of the testing method are sensitive to specimen and loading geometry and strain rate.

Calculation of the flexural stress σ_f

$$\sigma_f = \frac{3PL}{2bd^2}$$

Calculation of the flexural strain ε_f

$$\epsilon_f = \frac{6Dd}{L^2}$$

Calculation of Young's modulus E_B

$$E_B = \frac{L^3 m}{4bd^3}$$

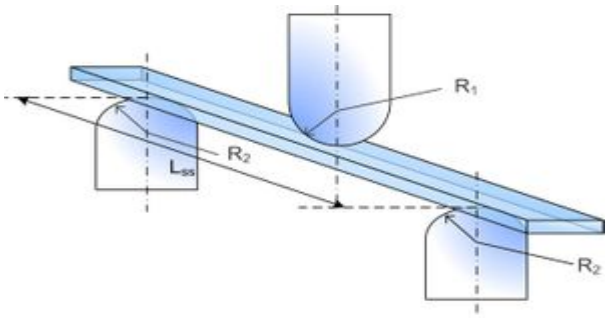

Fig2.5 3-Point Bending Test Setup

- σ_f = Stress in outer fibers at midpoint, [MPa]
- ε_f = Strain in the outer surface, [%]
- E_f = Modulus of elasticity in bending,[MPa]
- P = load at a given point on the load deflection curve, [N]
- L = Support span, [mm]
- b = Width of test beam, [mm]
- d = Depth of tested beam, [mm]
- D = maximum deflection of the center of the beam, [mm]
- m = Slope of the tangent to the initial straight-line portion of the load deflection curve, [N/mm]

2.5. FTIR-Imaging

The FTIR measuring principle is a measurement with IR light. Contrary to NDIR with a narrow wave length area by means of an optical filter, the scan area of the IR wave length by use of the FTIR measuring principle is large. The principle of FTIR is that the gas to be analyzed is led through a cuvette with an IR light source at one end that is sending out scattered IR light, and a modulator that "cuts" the infra red light into different wave lengths. At the other end of the cuvette a detector is measuring the amount of IR light to pass through the cuvette. Like the NDIR measuring principle it is the absorption of light at different wave lengths that is an expression of the concentration of gasses to be analyzed. By data processing, Fourier Transformation mathematics is used to turn the measured absorption values into gas concentrations for the analyzed gasses. As the light, when using the FTIR measuring principle, is modulated into many different wave lengths, it is possible to analyze many different gasses in the same instrument; such as CO, H_2O, SO_2, NO, NO_2, HCl, HF, NH_3.

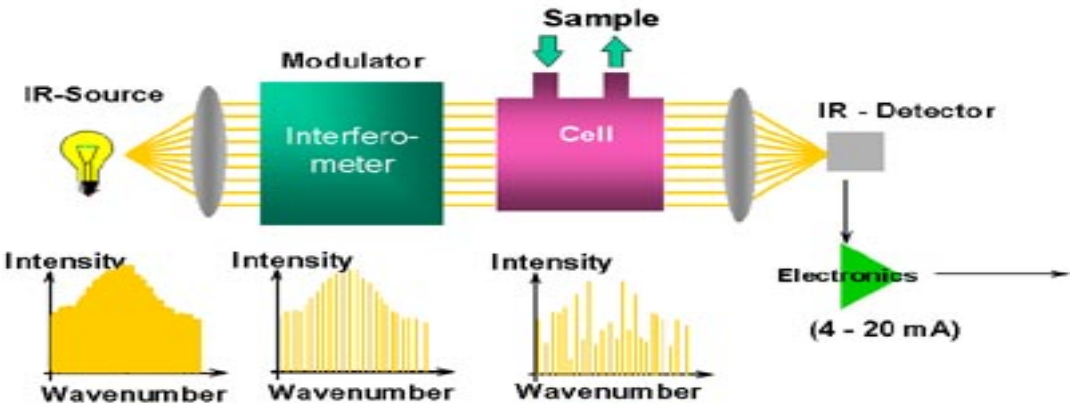

Fig2.6. FTIR-Imaging Principle

The FTIR microscope accessory allows spectra from a few nanograms of material to be obtained quickly, with little sample preparation, resulting in more data at lower cost. In some cases, thin films of residue are identified with a sensitivity that rivals or even exceeds electron or ion beam-based surface analysis techniques. There are few sample constraints; solids, liquids and gases can be accommodated. Many contaminants present on reflective surfaces such as solder pads or printed circuitry are readily analyzed in situ using the FTIR microscope in reflectance mode. FTIR spectroscopy is used primarily for qualitative and quantitative analysis of organic compounds, and also for determining the chemical structure of many inorganic compounds.

2.6 Scanning Electron Microscope

The Scanning Electron Microscope (SEM) is a microscope that uses electrons rather than light to form an image. There are many advantages to using the SEM instead of a light microscope. The SEM has a large depth of field, which allows a large amount of the sample to be in focus at one time. The SEM also produces images of high resolution, which means that closely spaced features can be examined at a high magnification. Preparation of the samples is relatively easy since most SEMs only require the sample to be conductive. The combination of higher magnification, larger depth of focus, greater resolution, and ease of sample observation makes the SEM one of the most heavily used instruments in research areas today.

In a typical SEM, electrons are thermionically emitted from a tungsten or lanthanum hexaboride (LaB_6) cathode and are accelerated towards an anode; alternatively, electrons can be emitted via field emission (FE). Tungsten is used because it has the highest melting point and lowest vapor pressure of all metals, thereby allowing it to be heated for electron emission. The electron beam, which typically has an energy ranging from a few hundred eV to 100 keV, is focused by one or two condenser lenses into a beam with a very fine focal spot sized 1 nm to 5 nm. The beam passes through pairs of scanning coils in the objective lens, which deflect the beam horizontally and vertically so that it scans in a raster fashion over a rectangular area of the sample surface. When the primary electron beam interacts with the sample, the electrons lose energy by repeated scattering and absorption within a teardrop-shaped volume of the specimen known as the interaction volume, which extends from less than 100 nm to around 5 μm into the surface, The size of the interaction volume depends on the beam accelerating voltage, the atomic number of the specimen and the specimen's density. The energy exchange between the electron beam and the sample results in the emission of electrons and electromagnetic radiation which can be detected to produce an image.

2.7. Work done by various persons on interphase study:

1. Interfacial Behavior of Epoxy/E-Glass Fiber Composites under Wet-Dry Cycles by FTIR Micro spectroscopy by W. NOOBUT and J. L. KOENIG, Department of Macromolecular Science Case, Western Reserve University Cleveland, Ohio 44 106

The interfacial behavior of epoxy/glass fiber micro-composites under cycles of wet and dry environment change was investigated by Fourier Transform Infrared (FTIR) micro spectroscopy. The adsorbed water content in the epoxy/fiber interphase under moist conditions is reduced by treating the glass fibers with a silane coupling agent, -y-aminopropyltriethoxysilane. This results in a significant decrease in the ring-opening polymerization of epoxy in the epoxy/fiber interphase. It is also found that the wet-dry cycles cause the significant variation of the residual adsorbed water in the interphase regions. There is an indication that the debonding in the epoxy/silane-treated fiber interphase is slower than the epoxy/heat-cleaned fiber interphase.

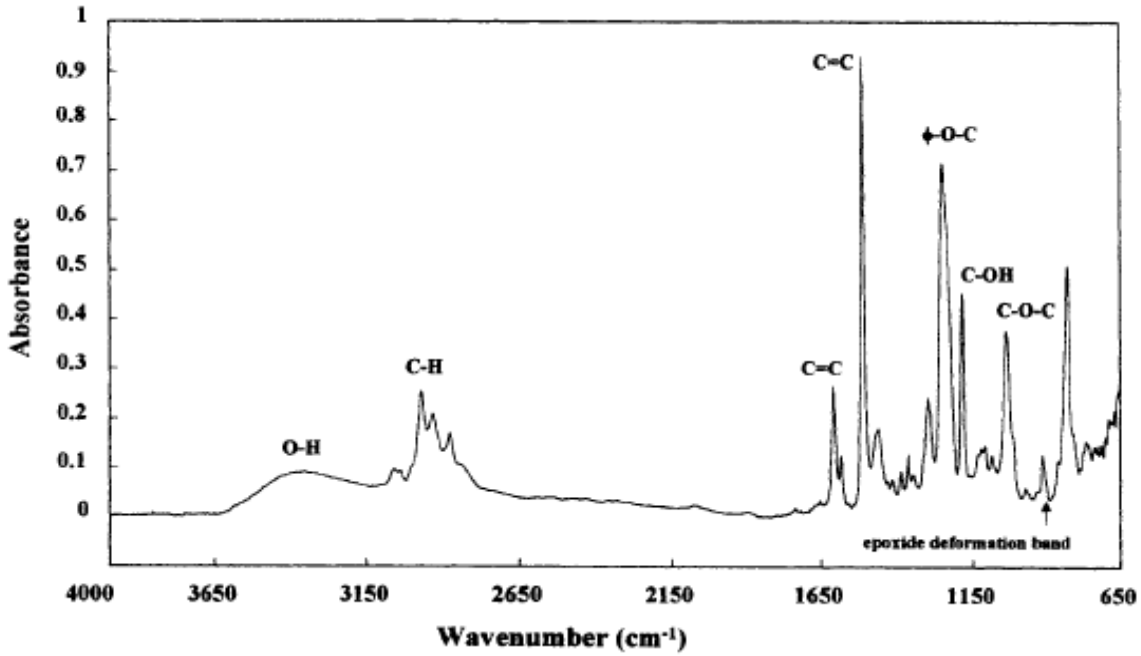

Fig 2.7 FTIR spectrum of bisphenol-A-based epoxy resin cured with tetraethylenepentamine.

Result

FTIR micro spectroscopy confirmed that the epoxy/ glass fiber interphase uptakes a lesser amount of water when the fiber is treated with a silane coupling agent. This results in the significant decrease of the additional ring-opening polymerization of epoxide groups in the

interphase. There was indication of slow debonding in the epoxy/APS-treated and epoxy/as-received glass fiber interphases relative to that of the epoxy/heat-cleaned fiber interphase. The rapid degradation of the interfacial properties of the composites is probably caused by the significant variation of the residual adsorbed water in the interphase region.

2. The nature of the structural gradient in epoxy curing at a glass fiber/epoxy matrix interface using FTIR imaging by J. Gonzalez-Benito, Department of Materials Science and Metallurgic Engineering, Universidad Carlos III de Madrid, Avda. Universidad 30, 28911 Leganes, Madrid, Spain

The curing process of an epoxide system was studied at the interface formed between a silane-coated glass fiber and an epoxy matrix. The gradient in the structure of the epoxy resin as a result of the cure process at the fiber/matrix interfacial region was monitored by FTIR imaging. For comparison, the epoxy curing at the interface formed between the epoxy resin and (a) an uncoated glass fiber and (b) a polyorganosiloxane (obtained from the silane used for the glass-fiber coating) were also monitored. Chemically specific images of the OH and the H–N–H groups near the interface region were obtained. These images suggest that there is a chemical gradient in the structure of the matrix from the fiber surface to the polymer bulk due to different conversions. The basis of the different kinetics of the curing reactions is a result of amino group inactivation at the interface. This deactivation translates into an off-stoichiometry of the reaction mixture, which is a function of the distance from the surface of the glass fiber.

Result

The curing process of an epoxy system at the interface formed with a silane coated glass fiber was studied by using FTIR imaging. Chemically specific images for OH and H–N–H within the system were obtained. The analysis of these images suggests that there is a variation in the chemical structure of the matrix from the fiber to the polymer bulk due to different conversions arising from a gradient in the initial composition. Furthermore, it was observed that the rate of the curing reaction changed depending on the distance to the glass fiber and this change was also associated to changes in the stoichiometry.

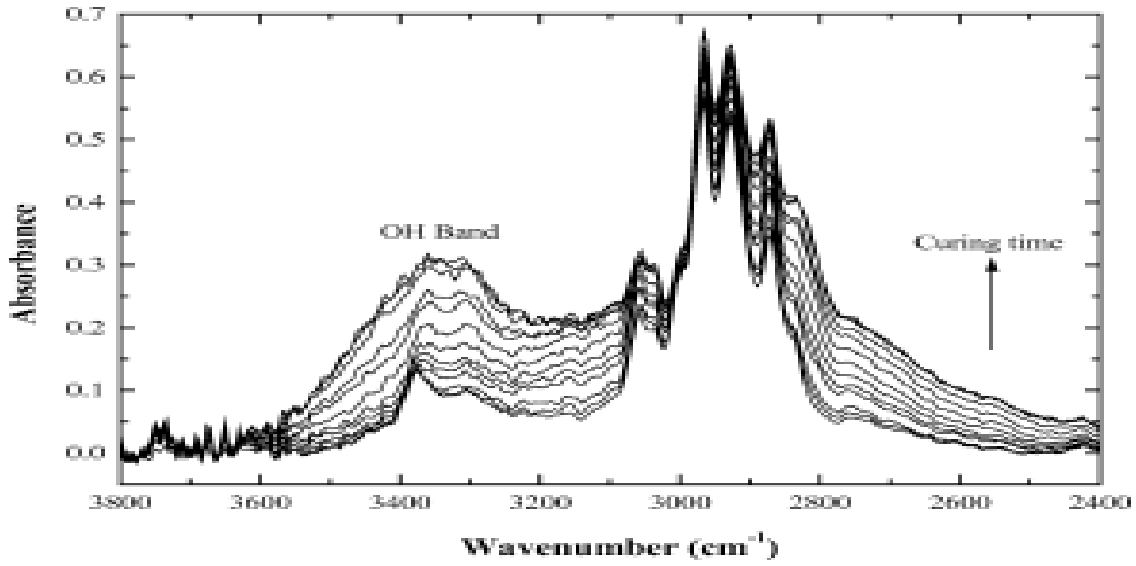

Fig 2.8. Evolution of the FTIR spectra for the epoxy–amine mixture as a function of the curing process.

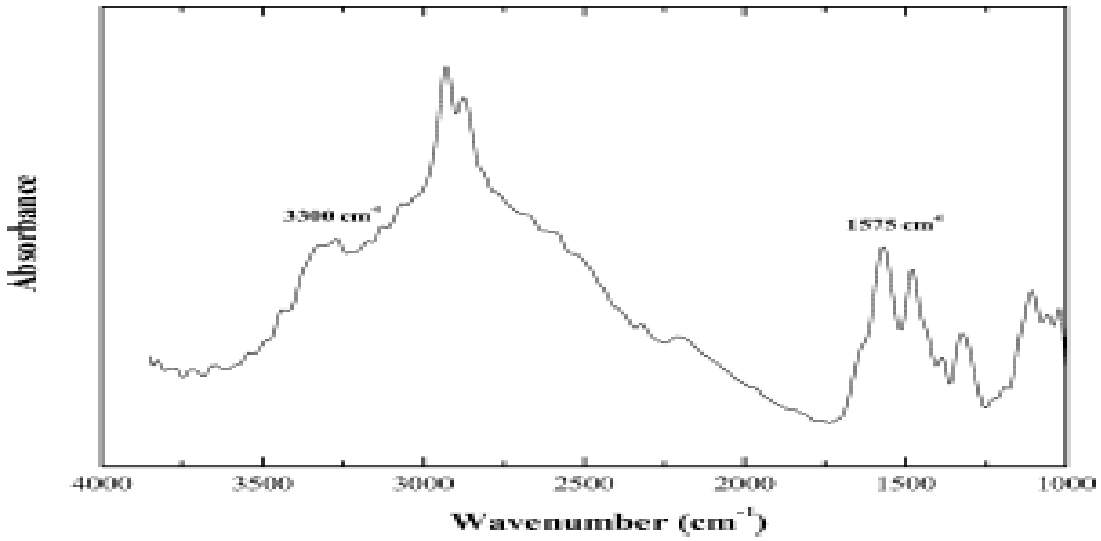

Fig 2.9. FTIR spectrum of the model poly (aminopropylsiloxane).

CHAPTER 3

EXPERIMENTAL PROCEDURE

3. EXPERIMENTAL PROCEDURE:

The procedure followed for carrying out our work consists of the following steps:

3.1. Fabrication and Cutting of the Composite:

The composite was fabricated using the conventional ***HAND LAYOUT*** method. The materials used are E-glass Fiber and Epoxy resin (araldite LY556). The hardener used is HY951. A sixteen layered structure was formed as per the ASTM standards. The fiber and the matrix were taken in the ratio of 50:50. The sample was left for drying for 24 hrs after the fabrication so that the matrix completely seeps in and become dry.

The samples were cut into the dimensions of 45mm X 6mm using diamond cutter and then the samples were oven dried to remove the water absorbed during cutting.

Fig 3.1. Composite sample after the final treatment

3.2. Hygrothermal Treatment:

The samples after cutting and oven drying were divided into 3 parts. One part is kept as such and was wrapped in Aluminium foil and stored in the dessicator after weighing all the samples. Second and third part were first weighed and then given a hygrothermal treatment by placing the samples in the Humidity chamber for 50 Hrs and 100 Hrs respectively at 50°C and 95% Humidity. The water level of the chamber was checked regularly in order to maintain the

humidity level. After the treatment is over, the samples were weighed again to calculate the amount of moisture absorbed.

Fig 3.2. Humidity Chamber

3.3. 3-Point Bend Test:

After the Hygrothermal treatment, the dimensions of all the samples were measured and then they were being tested for 3-Point bend test. This test was performed on INSTRON-1195. The samples were being loaded and the loading rate used were 2mm/min, 10mm/min, 50mm/min, 200mm/min, 500mm/min and the load vs. displacement graphs was obtained and then this graph was converted to stress vs. strain. From this graph, we calculated the ILSS value for all the specimens using the formula:

ILSS = (0.75 x P) / (W x T)

Where: P = Breaking load

W = Width of the specimen

T = Thickness of the specimen

3.4. Characterization By FTIR-Imaging:

The samples had fractured after 3-Point bend test and then samples were taken for FTIR-Imaging analysis from these samples. FTIR-Imaging was used to find out the changes that occurred due to moisture absorption at interface and also in the bulk of the matrix. One sample each of the dry, 50 Hr hygrothermal treatment, 100 Hr hygrothemal treatment were taken and then analyzed under the FTIR-Imaging machine.

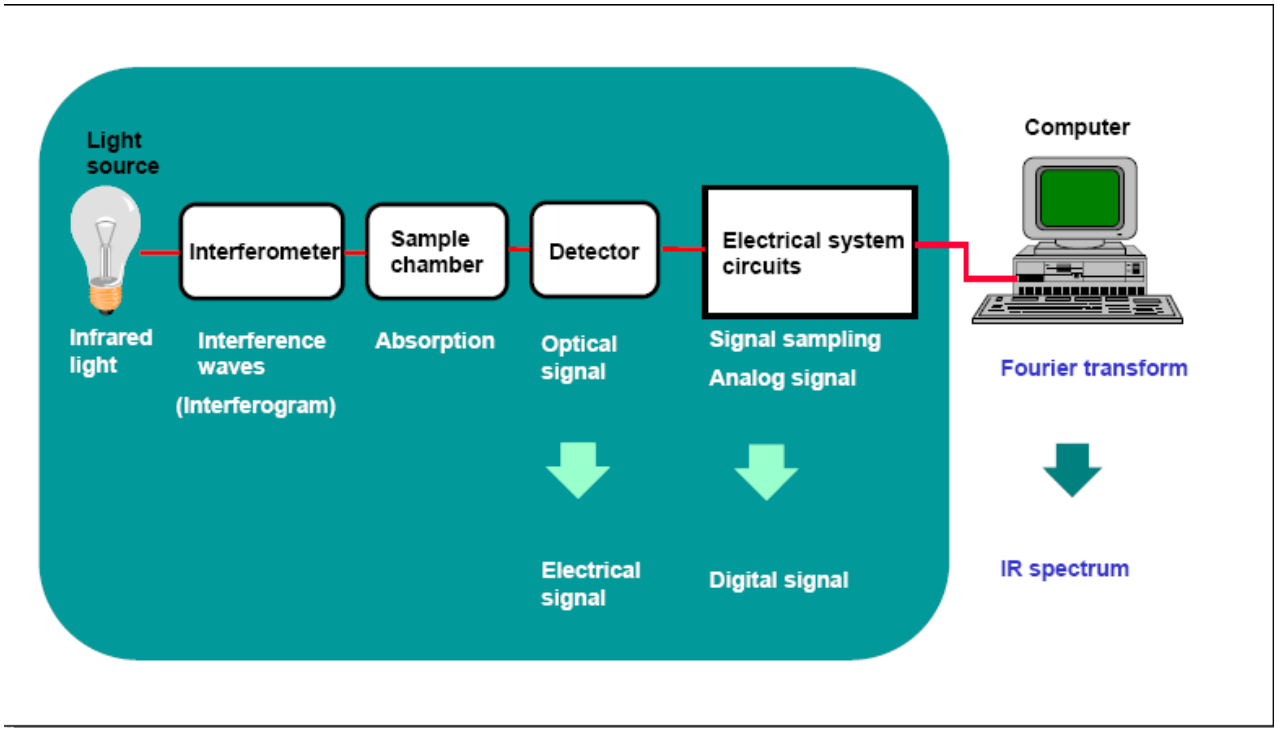

FIG 3.3. FTIR-Imaging working.

The FTIR-Imaging measures the amount of IR absorbed and gives the result in the form of graphs of absorbance vs. wave number. The working principle is that different functional groups have different values of wave number at which they absorb the IR so by finding out this value of wave number; we can predict the different functional groups present. By having an idea of the functional groups present in the samples that have given different treatment, we can find out the changes that have occurred due to the moisture absorption.

3.5. SEM of the fractured surfaces

To study the fracture surface of the samples being tested above, we carried out the SEM and these results helped us in the study of the effect of the moisture absorption at different positions.

Fig 3.4 Scanning Electron Microscope

The samples were first being loaded on the loading plate and then viewed under SEM to fix the positions of the plate. Vacuum level of the SEM chamber is being adjusted from time to time depending on the requirement. After that the samples were given coating of Platinum in order to make them conducting.

CHAPTER 4

RESULTS AND DISCUSSION

4. RESULTS AND DISCUSSION

4.1. Moisture Absorption

Sample no:	Initial weight (gms)	Final weight (gm)	% Moisture absorbed
1	3.7632	3.7632	0
2	4.3281	4.3281	0
3	3.6738	3.6738	0
4	4.3017	4.3017	0
5	3.5323	3.5323	0
6	3.5016	3.5016	0
7	3.9112	3.9112	0
8	3.0288	3.0288	0
9	3.3892	3.3892	0
10	3.9215	3.9215	0

Sample no:	Initial weight (gms)	Final weight (gm)	% Moisture absorbed
11	4.2998	4.2998	0
12	3.5447	3.5447	0
13	3.5243	3.5243	0
14	4.3713	4.3713	0
15	3.8762	3.8762	0
16	3.3201	3.3201	0
17	3.6752	3.6752	0
18	3.5942	3.5942	0
19	3.5594	3.5594	0
20	3.6591	3.6591	0

Table 4.1 & 4.2. Moisture Absorption in Case of Dry Samples.

Sample no:	Initial weight (gms)	Final weight (gm)	% Moisture absorbed
21	2.6657	2.6932	1.031
22	2.9087	2.9408	1.103
23	3.7362	3.7755	1.051
24	3.4543	3.4893	1.103
25	5.1186	5.1642	0.89
26	3.2302	3.2624	0.996
27	3.9903	4.0311	1.02
28	3.3669	3.4031	1.075
29	3.8369	3.8769	1.042
30	3.6393	3.6784	1.074

Sample no:	Initial weight (gms)	Final weight (gm)	% Moisture absorbed
31	3.4853	3.5223	1.061
32	3.8057	3.8484	1.122
33	3.6389	3.6776	1.063
34	4.1708	4.2158	1.078
35	3.2235	3.2596	1.119
36	3.8104	3.8492	1.018
37	4.1304	4.1942	1.544
38	4.5596	4.5985	0.853
39	3.3641	3.3964	0.960
40	3.6022	3.6417	1.096

Table 4.3 & 4.4. Moisture Absorption in case of 50 Hrs Hygrothermal Treated Samples

Sample no:	Initial weight (gms)	Final weight (gm)	% Moisture absorbed
41	*3.6120*	*3.6592*	*1.306*
42	*4.2046*	*4.2474*	*1.017*
43	*3.6762*	*3.7210*	*1.218*
44	*3.8358*	*3.8815*	*1.191*
45	*3.6614*	*3.7050*	*1.190*
46	*3.6513*	*3.6934*	*1.177*
47	*3.7266*	*3.7710*	*1.191*
48	*3.6492*	*3.6933*	*1.208*
49	*3.7408*	*3.7846*	*1.170*
50	*3.8448*	*3.8910*	*1.201*

Sample no:	Initial weight (gms)	Final weight (gm)	% Moisture absorbed
51	*3.8582*	*3.9048*	*1.207*
52	*3.0928*	*3.1292*	*1.176*
53	*4.0574*	*4.1080*	*1.247*
54	*3.7572*	*3.8021*	*1.195*
55	*3.7585*	*3.8037*	*1.202*
56	*3.5894*	*3.6329*	*1.211*
57	*3.7496*	*3.7932*	*1.162*
58	*3.5921*	*3.6304*	*1.066*
59	*3.6923*	*3.7359*	*1.180*
60	*3.1450*	*3.1828*	*1.201*

Table 4.5 & 4.6 Moisture Absorption in case of 100 Hrs Hygrothermal treated samples.

These above results can be formulated in the forma of a table as under.

S.NO	No. of Hours of Hygrothermal treatment (Hrs)	Average moisture absorbed (%)
1	0	0
2	50	1.07
3	100	1.19

Table 4.7. Average moisture absorbed.

This table can be represented in the form of a graph and from that graph we can interpret about the moisture absorption in the treatment given.

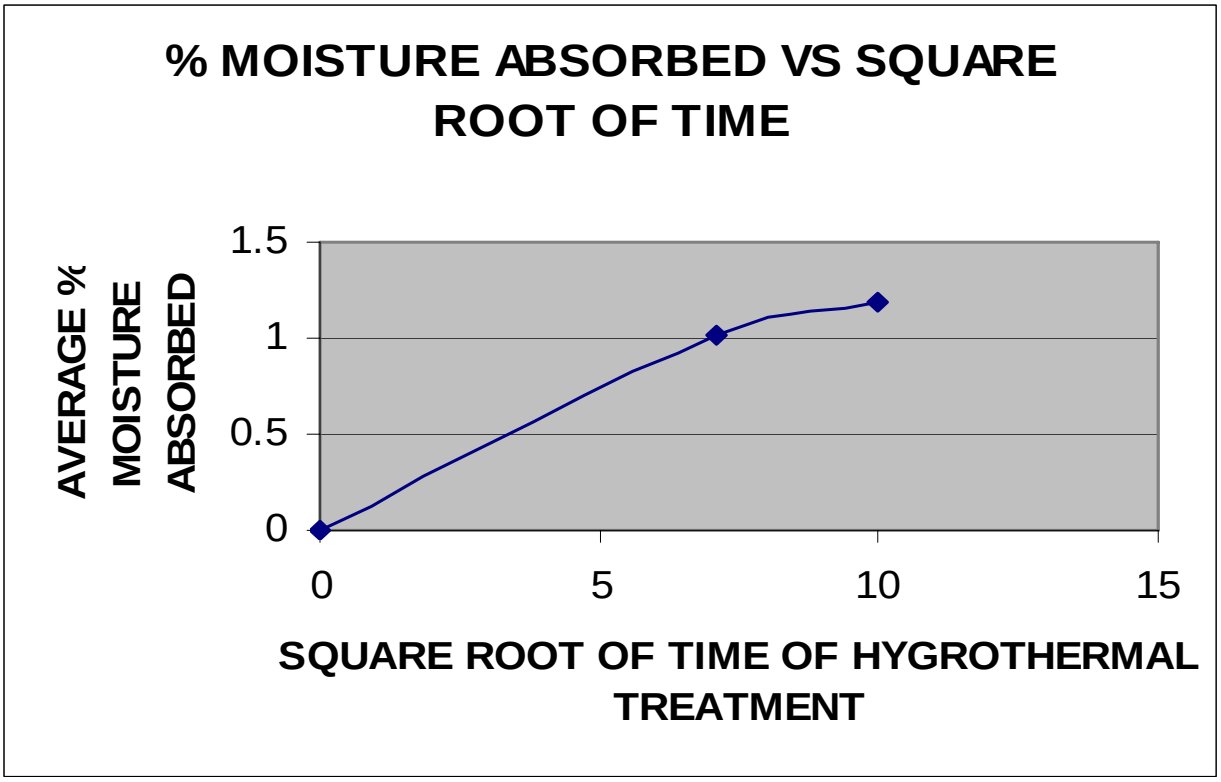

Fig 4.1 Graph between average moisture absorbed and square root of time

Interpretation

From the above graph we can interpret the following points.

- Initially the rate of moisture absorption is high. This is due to the presence of free spaces in the composites. The moisture absorption obeys fick's law i.e. the fickian curve is obtained.
- After a specific time the rate of moisture absorption decreases gradually. This is due to the saturation of the matrix i.e. the moisture absorbed is sufficient enough to fill the spaces and very less moisture is required.
- So we can conclude that moisture absorption is highest in the beginning and the gradually goes on decreasing after a specific interval of time due to saturation.

4.2. Effect of Rate of Loading on ILSS

1. Dry Sample

Specimen no:	Crosshead velocity (mm/min)	Stress at yield (kg/mm2)	Load at yield (kg)	ILSS (kg/mm2)	Avg. ILSS (kg/mm2)
1	2	14.71	153.2	1.86	1.94
2		16.81	181.2	2.05	
3		16.32	160.4	1.99	
4		13.85	168.1	1.86	
5	10	17.18	152.8	2.12	2.02
6		17.12	149.2	2.03	
7		17.69	165.1	2.12	
8		14.18	111.3	1.81	
9	50	15.12	137.3	1.86	1.92
10		19.01	186.5	2.32	
11		14.68	185.5	2.03	
12		12.29	108.6	1.45	
13	200	16.74	141.8	1.92	1.87
14		14.19	182.8	1.99	
15		17.78	171.0	2.13	
16		11.62	106.0	1.44	
17	500	14.78	147.0	1.85	1.74
18		14.34	143.4	1.78	
19		16.71	137.8	1.88	
20		11.36	118.8	1.45	

Table 4.8 ILSS calculation for Dry Sample at different loading rates.

This table shows the variation of ILSS value for the dry samples with the change in loading rates and these results can be represented in the form of a graph between the Average ILSS value vs. crosshead velocity.

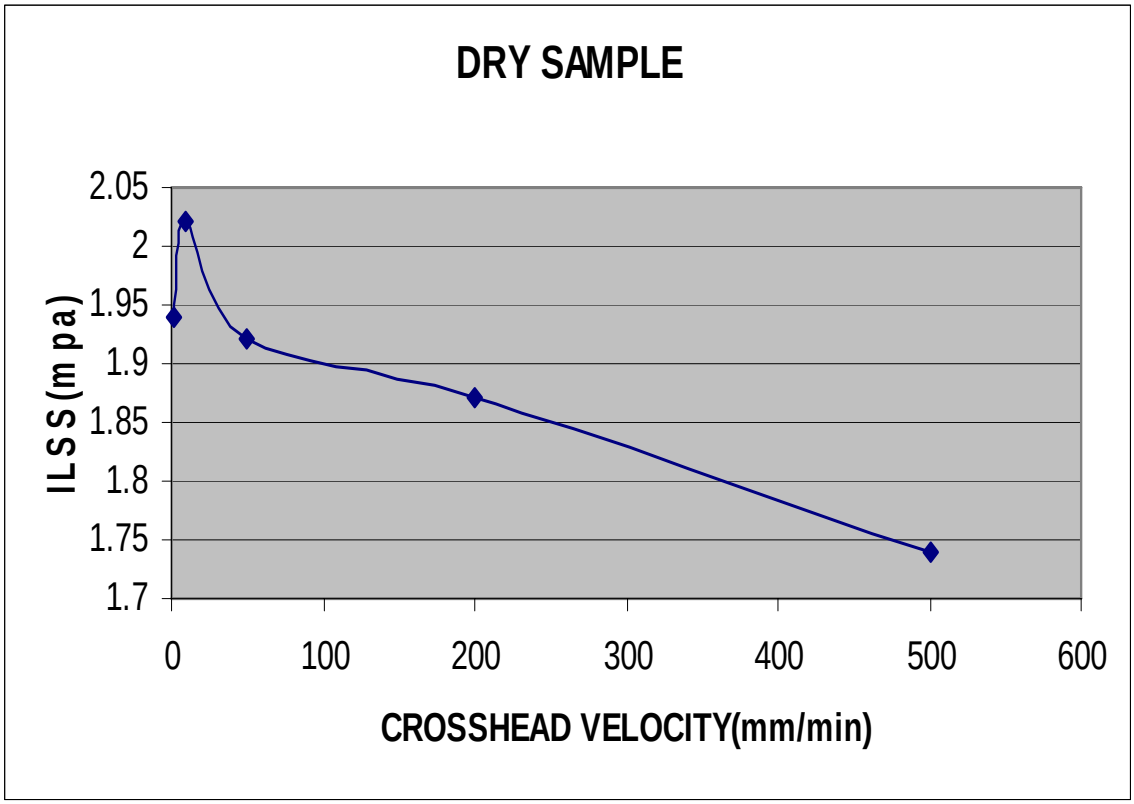

Fig 4.2. Variation of Average ILSS Value with Crosshead Velocity for Dry sample

Interpretation

- From the above graph, it is clear that the ILSS value first increases with the increase in the crosshead velocity and then after 10mm/min, it decreases.
- The ILSS value is low at low strain rate as the load applied on the specimen is held for more time and thus more deterioration will take place and the material will fail at a low ILSS value
- The ILSS value is also low at high rate as very less time is available for the transfer of load from fiber to matrix and the load applied acts as a impact and thus the material fails at a low ILSS value.
- Thus from above we can conclude that the loading rate should neither be low nor high but it should be kept optimum so that proper time is available for the transfer of load from fiber to matrix and also the load is not applied on the material for more time.
- Here the optimum loading is found out to be 10mm/min.

2. 50 Hrs Hygrothermally Treated sample

Specimen no:	Crosshead velocity (mm/min)	Stress at yield (kg/mm2)	Load at yield (kg)	ILSS (kg/mm2)	Avg. ILSS (kg/mm2)
21	2	13.81	110.7	1.72	1.75
22		14.91	147.1	1.84	
23		17.66	131.7	1.94	
24		9.39	174.2	1.48	
25	10	14.46	124.9	1.71	1.84
26		17.86	177.4	2.19	
27		9.73	114.4	1.38	
28		16.65	168.2	2.06	
29	50	16.53	165.5	2.07	2.04
30		16.86	146.6	2.01	
31		14.42	161.4	2.04	
32	200	19.63	192.0	2.43	1.97
33		8.93	110.1	1.23	
34		15.0	145.4	2.00	
35		17.63	183.3	2.23	
36	500	15.83	158.8	1.92	1.75
37		15.25	240.2	2.32	
38		6.505	71.19	0.84	
39		12.94	136.2	1.68	

Table 4.9 ILSS calculation for 50 Hrs Hygrothermally treated sample at different loading rates.

This table shows the variation of ILSS value for the 50 Hrs Hygrothermally treated samples with the change in loading rates and these results can be represented in the form of a graph between the Average ILSS value vs. crosshead velocity.

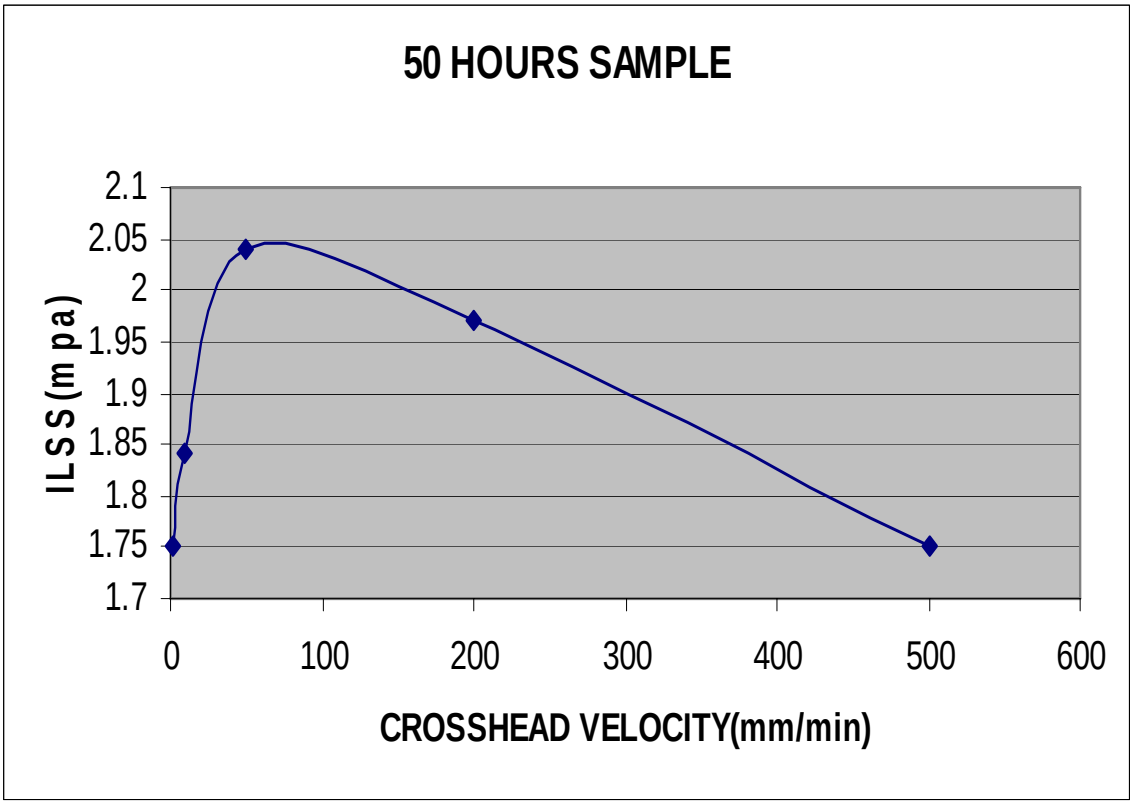

Fig 4.3 Variation of Average ILSS Value with Crosshead Velocity for 50 Hrs Hygrothermally Treated Sample

Interpretation

- From the above graph, it is clear that the ILSS value first increases with the increase in the crosshead velocity and then after 50mm/min, it decreases.
- The ILSS value is low at low strain rate as the load applied on the specimen is held for more time and thus more deterioration will take place and the material will fail at a low ILSS value
- The ILSS value is also low at high rate as very less time is available for the transfer of load from fiber to matrix and the load applied acts as a impact and thus the material fails at a low ILSS value.
- Thus from above we can conclude that the loading rate should neither be low nor high but it should be kept optimum so that proper time is available for the transfer of load from fiber to matrix and also the load is not applied on the material for more time.
- Here the optimum loading is found out to be 50mm/min.

3. 100 Hrs Hygrothermally Treated sample

Specimen no:	Crosshead velocity (mm/min)	Stress at yield (kg/mm2)	Load at yield (kg)	ILSS (kg/mm2)	Avg. ILSS (kg/mm2)
41	2	15.14	159.9	1.97	1.86
42		12.85	178.9	1.88	
43		11.95	137.4	1.65	
44		15.25	156.3	1.92	
45	10	18.33	182.0	2.27	1.95
46		12.86	142.6	1.68	
47		15.46	162.5	1.95	
48		13.92	153.3	1.90	
49	50	19.11	194.7	2.40	2.10
50		18.76	178.8	2.27	
51		19.19	191.6	2.36	
52		9.34	109.1	1.37	
53	200	15.25	185.9	2.14	2.00
54		16.34	165.9	2.02	
55		16.09	155.2	1.97	
56		16.04	137.2	1.85	
57	500	14.59	146.5	1.81	1.62
58		13.57	108.6	1.46	
59		14.13	151.6	1.82	
60		10.40	105.5	1.37	

Table 4.10 ILSS calculation for 100 Hrs Hygrothermally treated sample at different loading rates.

This table shows the variation of ILSS value for the 100 Hrs Hygrothermally treated samples with the change in loading rates and these results can be represented in the form of a graph between the Average ILSS value vs. crosshead velocity.

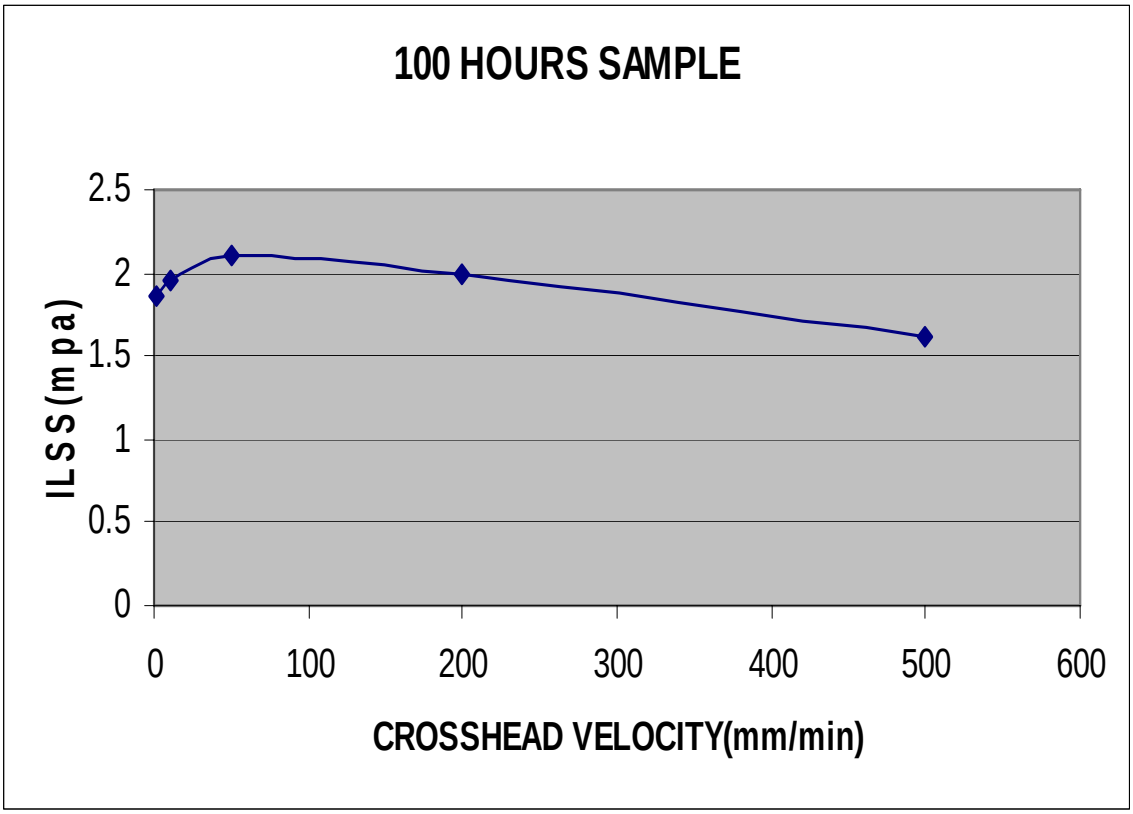

Fig 4.4 Variation of Average ILSS Value with Crosshead Velocity for 100 Hrs Hygrothermally treated sample

Interpretation

- From the above graph, it is clear that the ILSS value first increases with the increase in the crosshead velocity and then after 50mm/min, it decreases.
- The ILSS value is low at low strain rate as the load applied on the specimen is held for more time and thus more deterioration will take place and the material will fail at a low ILSS value
- The ILSS value is also low at high rate as very less time is available for the transfer of load from fiber to matrix and the load applied acts as a impact and thus the material fails at a low ILSS value.
- Thus from above we can conclude that the loading rate should neither be low nor high but it should be kept optimum so that proper time is available for the transfer of load from fiber to matrix and also the load is not applied on the material for more time.
- Here the optimum loading is found out to be 50mm/min.

4.3. Effect of Moisture Content on ILSS

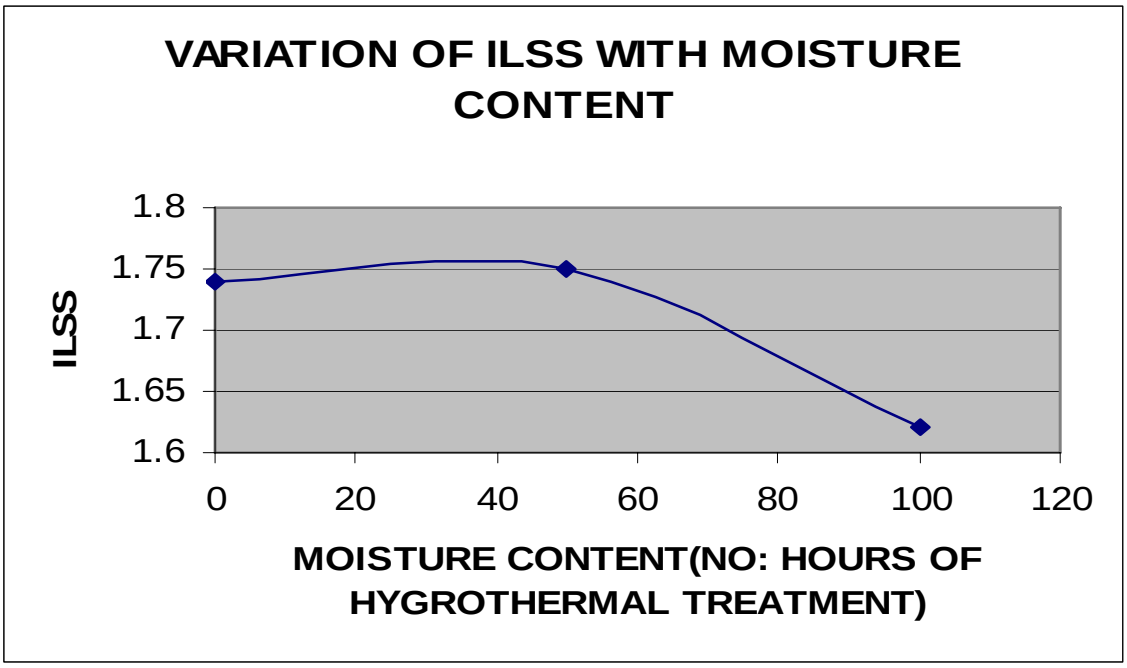

Fig 4.5 Variation of ILSS value with the moisture absorption (No. of Hrs of Hygrothermal Treatment)

Interpretation

From the above graph we came to the following inferences:

- Initial moisture level increases the ILSS values. This may be due to the relief of the stresses induced during curing.
- There results swelling stresses due to the expansion of the matrix by moisture absorption---these are opposite in nature to the curing stresses. Hence ILSS increases.
- With subsequent moisture absorption, ILSS decreases because the adhesion between the molecules is lowered.

4.4. FTIR-Imaging Characterization Results

1. Dry Sample Results

Fig 4.6 FTIR-Images for Dry Sample

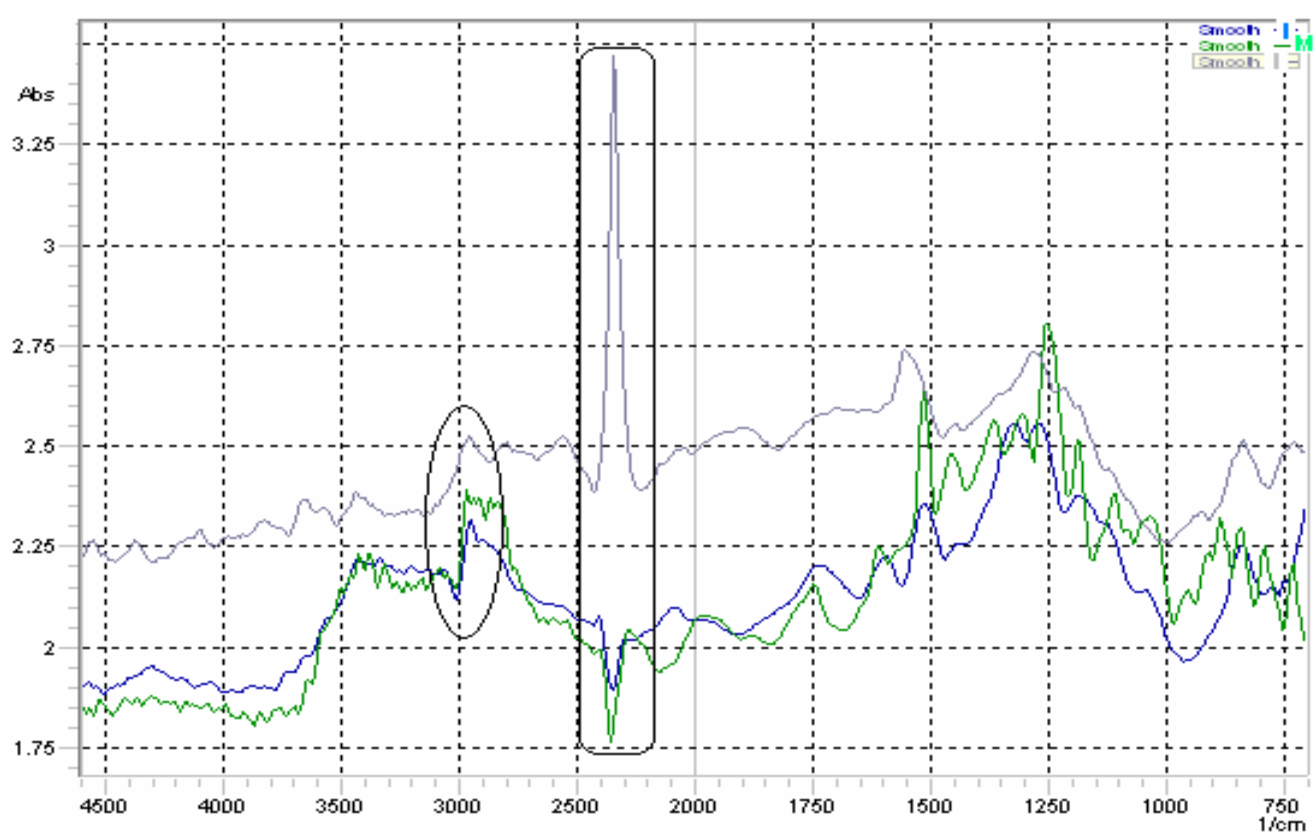

Fig 4.7 Absorbance vs. Wave number Graph for Dry Sample

Interpretation

- The graph under the ellipse shows the region for the OH stretching bond and the Rectangular region shows the COOH debonding region.
- The moisture absorption is more in the inner interface and decrease to the outer interface.
- The moisture is absorbed in this case is due to exposure to water during cutting of the samples.

- The moisture content is more in the inner Interface as the moisture from outer interface and the matrix is removed when the sample was dried in oven.
- The debonding has occurred in the outer interface and the matrix, so the moisture absorbed is more in the inner interface.
- The debonding results in the formation of voids or free surfaces and thus the diffusion of water becomes easier and it seeps into the inner interface through matrix.

2. 50 Hrs Hygrothermally treated samples results

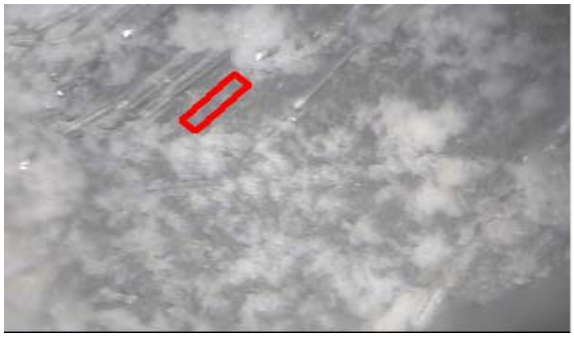

Fig 4.8 FTIR-Image for 50 Hrs Hygrothermally treated sample

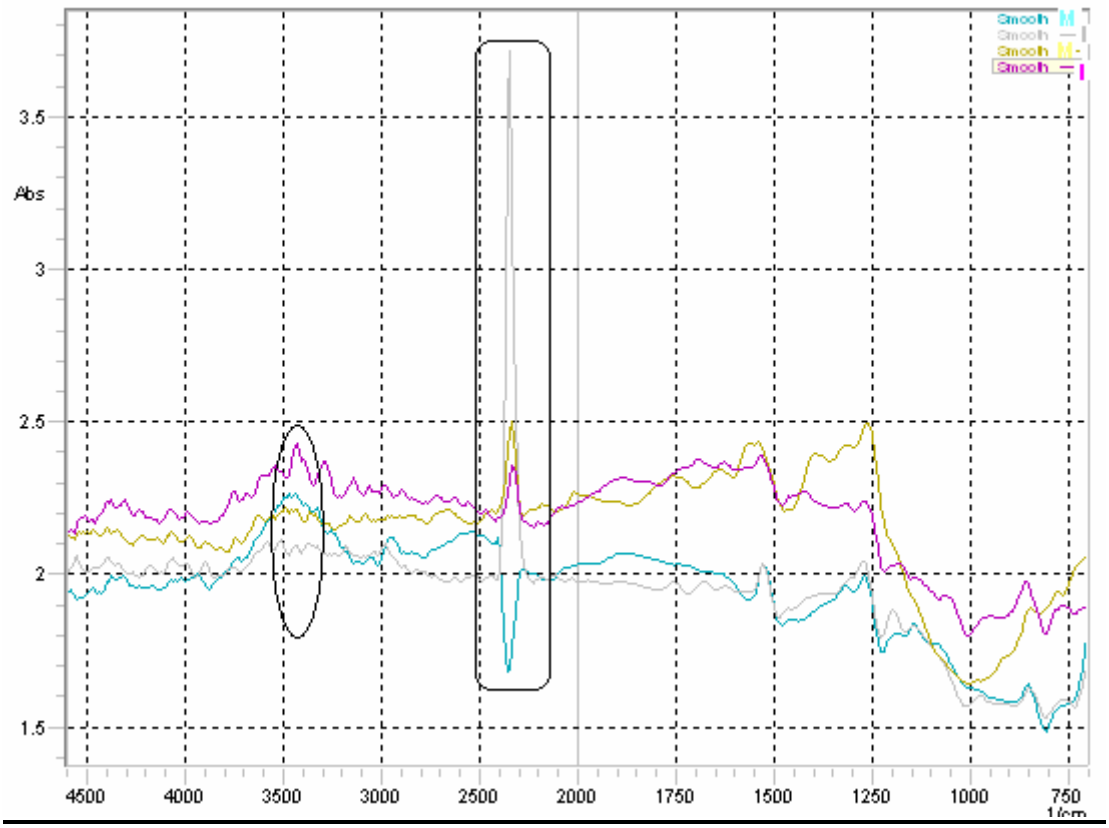

Fig 4.9 Absorbance vs. Wave number Graph for 50Hrs Hygrothermally treated Sample

Interpretation

- The graph under the ellipse shows the region for the OH stretching bond and the Rectangular region shows the COOH debonding region.
- The moisture absorption is more in the outer interface and decrease to the inner interface.
- The moisture content is more in the outer interface due to the presence of voids present in the samples and also the ability of the matrix to absorb moisture is more in the beginning.
- The debonding has occurred in the matrix, so the moisture has moved inside the matrix. Two regions have formed in the matrix and they are differentiated by the amount of the moisture absorbed.
- The debonding results in the formation of voids or free surfaces and thus the diffusion of water becomes easier and it seeps into the inner interface through matrix.
- The moisture absorbed is more at the interface and less in the matrix due to the ability of the interface to absorb moisture as it contains voids and free surfaces.

3. 100 Hrs Hygrothermally treated samples results

Fig 4.10 FTIR-Image for 100 Hrs Hygrothermally treated sample

From the above image, it is clear that the moisture absorption has taken place and has affected the matrix and due to moisture absorption, the matrix is appearing in two colors.

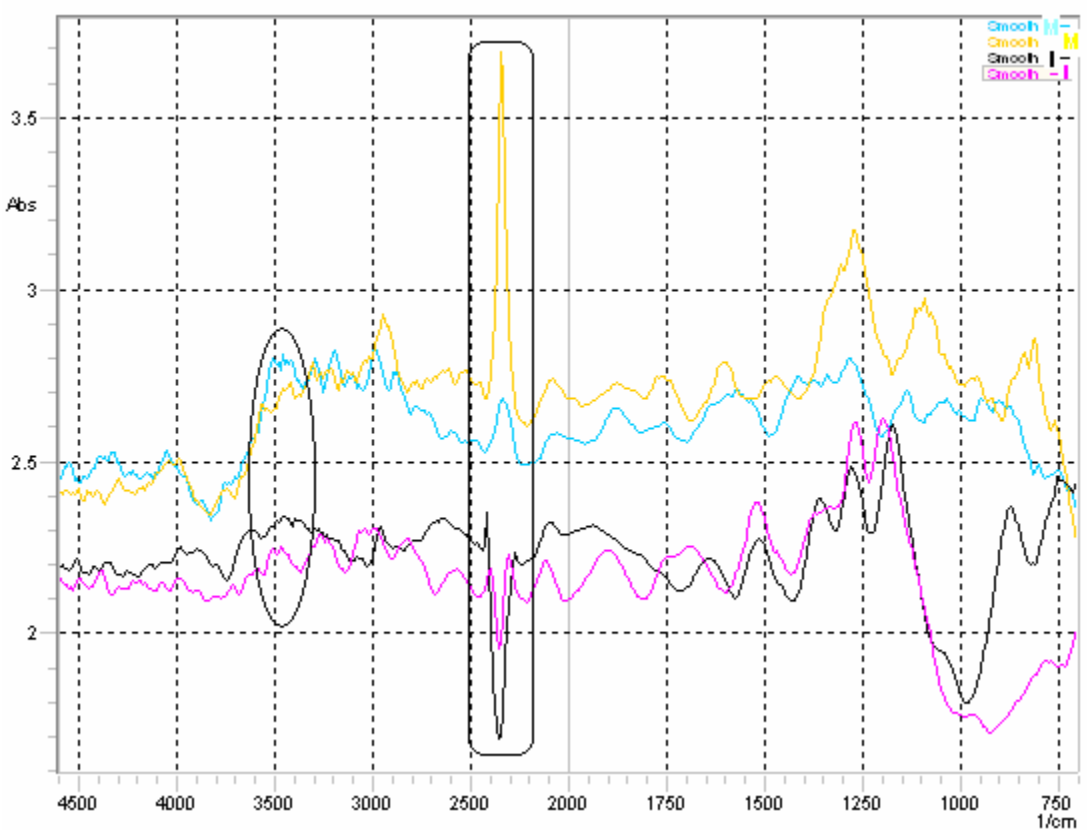

Fig 4.11 Absorbance vs. Wave number Graph for 100Hrs Hygrothermally treated Sample

Interpretation

- The graph under the ellipse shows the region for the OH stretching bond and the Rectangular region shows the COOH debonding region.
- The moisture absorption is more in the matrix and decreases from the inner interface to outer interface.
- The moisture content is more in the matrix due to the debonding in the interface which has resulted in the creation of voids and thus the moisture diffuses into the matrix. The moisture absorbed has resulted in the change of color of matrix.
- The debonding results in the formation of voids or free surfaces and thus the diffusion of water becomes easier and it seeps into the matrix from the interface.
- The moisture absorbed is more at the matrix and less in the interface as the debonding has occurred only in the interface and not the matrix.

4. Comparison of the Interface Behavior

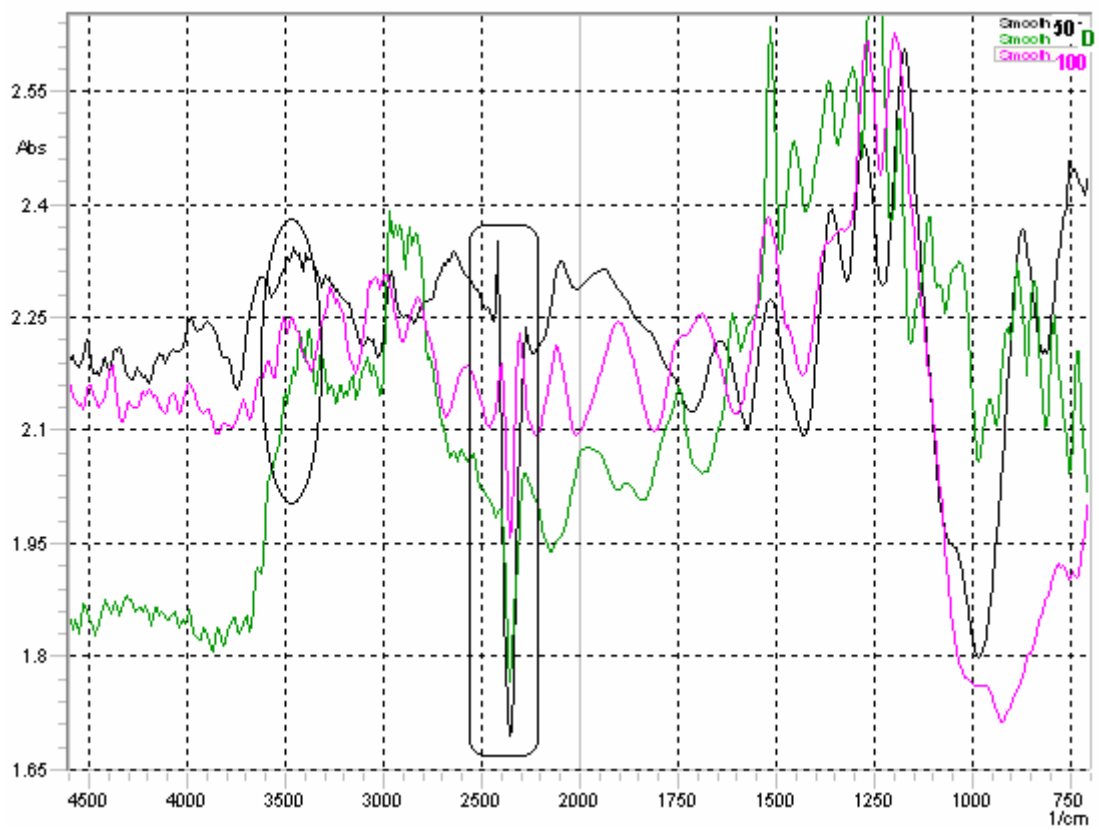

Fig 4.12. Absorbance vs. Wave number Graph for interface behavior of the different samples.

Interpretation

- The graph under the ellipse shows the region for the OH stretching bond and the Rectangular region shows the COOH debonding region.
- The moisture absorption is more in the case of 50 Hrs treated sample and then 100 Hrs treated sample and less in Dry sample.
- The moisture content is more in the interface of 50 Hrs sample as the debonding has not taken place in the interface whereas debonding has occurred in case of the 100 Hrs treated sample that has resulted in the creation of voids and thus the moisture diffuses into the matrix.

5. Comparison of the Matrix Behavior

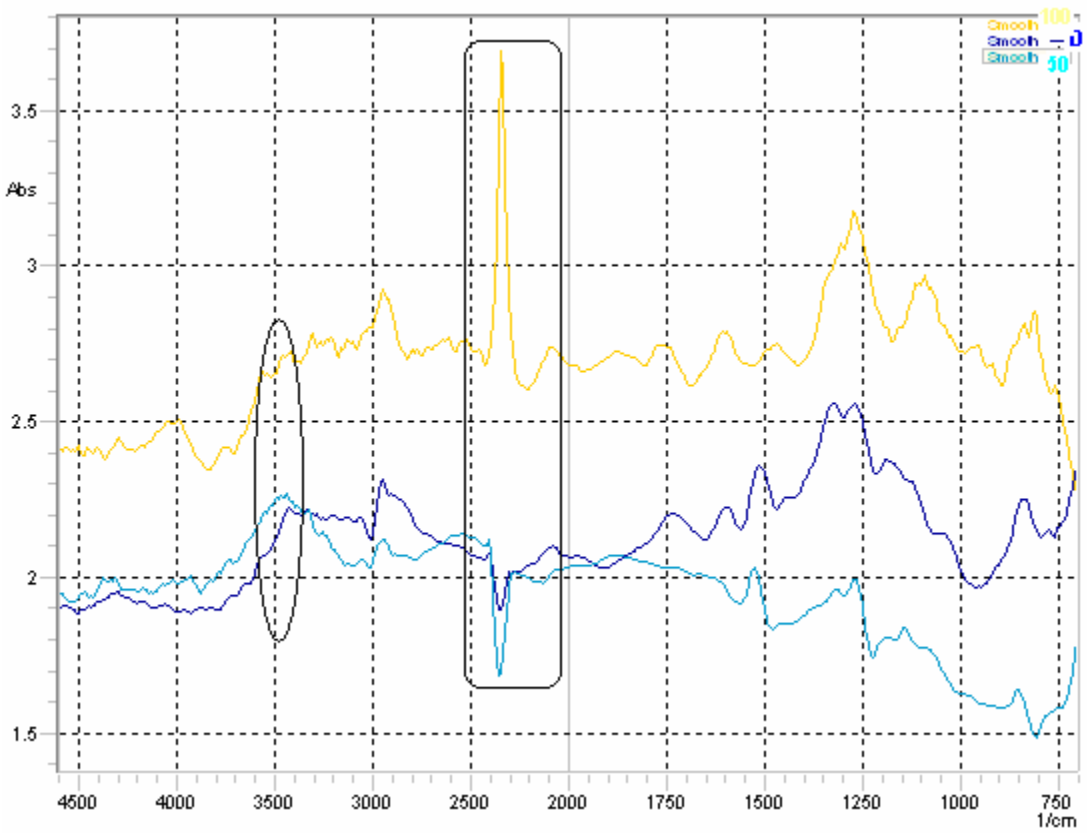

Fig 4.13. Absorbance vs. Wave number Graph for matrix behavior of the different samples

Interpretation

- The graph under the ellipse shows the region for the OH stretching bond and the Rectangular region shows the COOH debonding region.
- The moisture absorption is more in the case of 100 Hrs treated sample and then 50 Hrs treated sample and less in Dry sample.
- The moisture content is more in the matrix of 100 Hrs sample as the debonding has occurred at the interface in case of the 100 Hrs treated sample that has resulted in the creation of voids and thus the moisture diffuses into the matrix.
- The moisture absorbed is less at in the matrix of the 50 Hrs sample as the some amount of debonding has occurred in the matrix itself and the water that gets absorbed diffuses to the inner interface.
- The debonding results in the creation of voids or free surfaces so that water can easily diffuse in and enter the region next to the debonded region.

4.5. Scanning Electron Microscope Results

1. Dry Sample

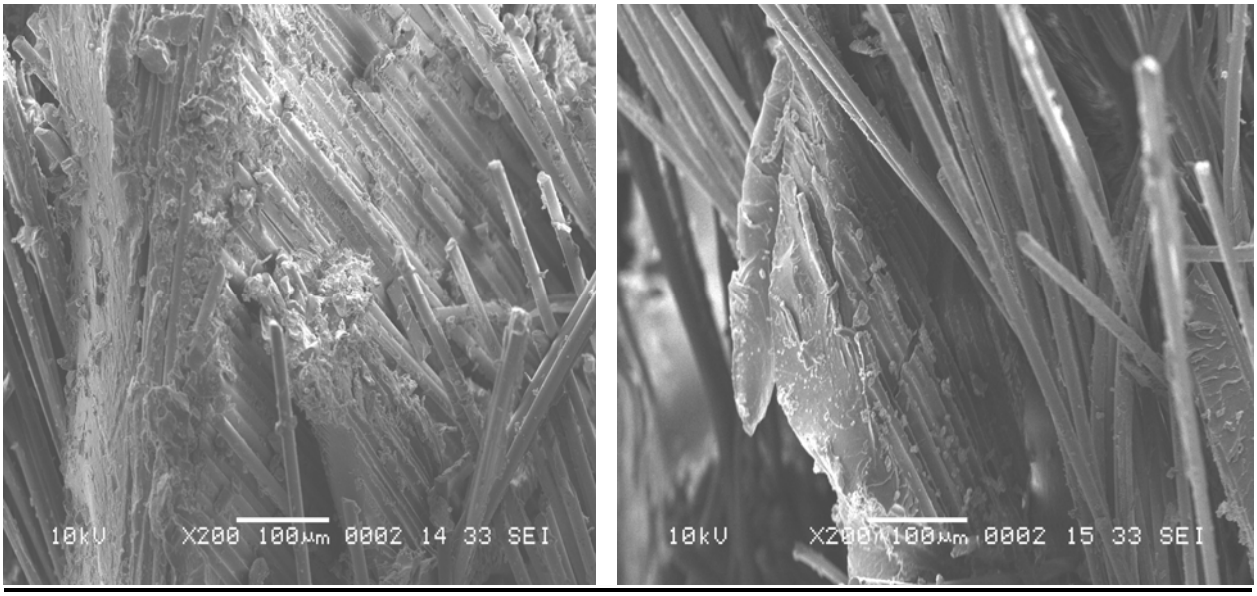

Fig 4.14. SEM Images of the fractured surface of Dry sample.

Interpretation

- From the above Images, it is clear that the matrix is strongly bonded to the fibers at the interface and this result in the increase of strength and fracture is ductile.
- Some amount of moisture absorbed during cutting has resulted in the removal of matrix from the interface and thus decreasing strength at those points.

2. 50 Hrs Hygrothermally treated Sample

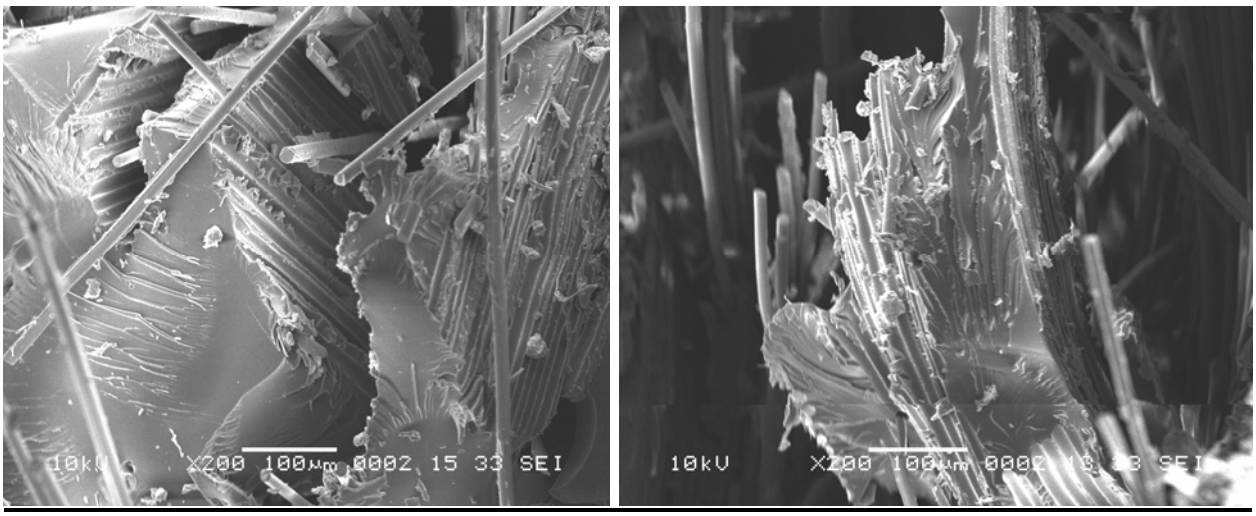

Fig 4.15. SEM Images of the fractured surface of 50 Hrs Hygrothermally treated sample.

Interpretation

- From the above Images, it is clear that the matrix has squeezed due to the moisture absorption and increases the bonding between fibers and matrix and this result in the increase of ILSS value and ductile fracture results.
- Due to moisture absorption some of the fibers have loosen contact with the matrix and thus this results in the decrease of strength.
- The overall result of the two is increase of the ILSS value.

3. 100 Hrs Hygrothermally treated Sample

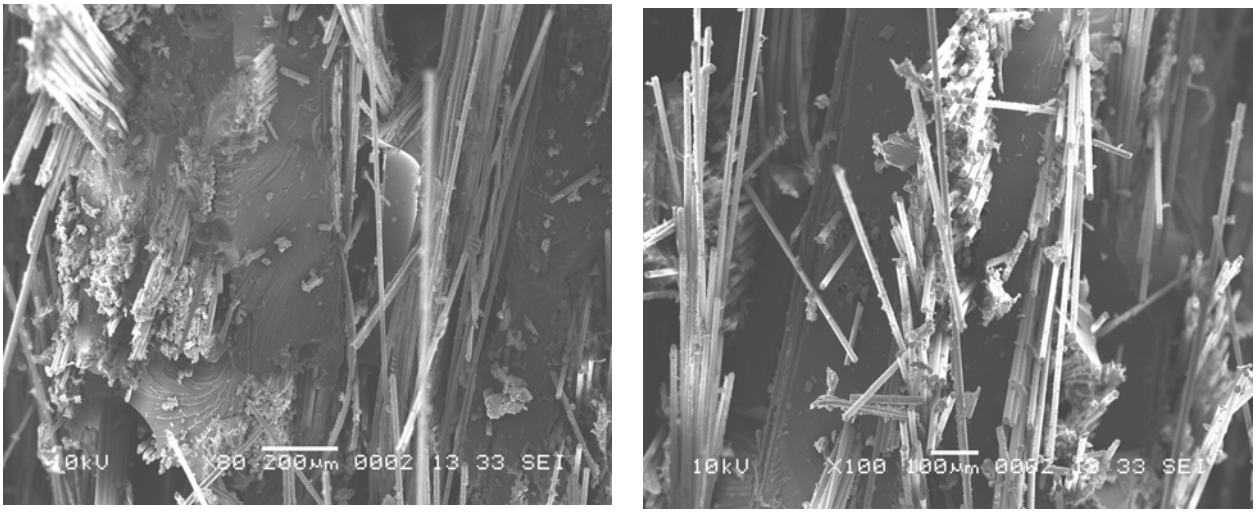

Fig 4.16. SEM Images of the fractured surface of 100 Hrs Hygrothermally treated Sample.

Interpretation

- From the above Images, it is clear that the matrix has loosen contact with the fiber due to moisture absorption and this has occurred due to the debonding at the interface and this results in the decrease of ILSS value.
- The fibers have completed lost contact with the other fibers and the matrix. The matrix-matrix bonding is also diminished.
- The above two factors results in the decrease of the ILSS value.

CHAPTER 5

CONCLUSION

5. CONCLUSION

- The ILSS value increases with initial moisture absorption due to the relief of residual stresses but after a certain stage it decreases due to the loss of adhesion between matrix and fiber.
- The ILSS value increases with the strain rate but after a certain stage it decreases because the matrix is unable to transfer load properly i.e. ILSS value is low at low strain rate as well as high strain rate as at low strain the load is applied for more time and thus the specimen fails at low stress value and at high strain rate, the time available for transfer of load is insufficient and the load acts as an impact and thus specimen fails at low stress. Thus the rate of loading should be optimum.
- From the FTIR-IMAGING Results, it is clear that the moisture absorption is more at the interface in low Hrs treatment as the components of composites have the property to absorb moisture and then moisture absorption is more in matrix due to more debonding leading to creation of voids at the interface and thus the water diffuses in easily through the interface to matrix.
- From the SEM Images of the fractured surfaces, it is clear that the initial moisture absorption results in the increase in the bond strength as the matrix gets squeezed but after a saturation stage, the moisture absorption results in the debonding of the matrix-interface bond and also matrix-matrix bond and thus ILSS value initially increases and then decreases.

REFERENCES

1. J. Gonzalez-Benito - The nature of the structural gradient in epoxy curing at a glass fiber/epoxy matrix interface using FTIR imaging, Journal of Colloid and Interface Science 267 (2003) 326–332.
2. Z.A. Mohd. Ishak, B.N. Yow, H. P. S. A. Khalil, H.D. Rozman - Hygrothermal Aging and Tensile Behavior of Injection-Molded Rice Husk-Filled Polypropylene Composites, *Journal of Applied Polymer Science*, 81(14), 2000, 742-753.
3. B.N. Yow, U.S. Ishiaku, Z.A. Mohd Ishak, J. Karger-Kocsis - Kinetics of Water Absorption and Hygrothermal Aging Rubber Toughened Poly(Butylene Terephthalate) With and Without Short Glass Fiber Reinforcement, *Composites Science and Technology*, 60(6), 2003, 803-815.
4. B.F. Boukhoulda, E. Adda-Bedia, K. Madani - The Effect of Fiber Orientation Angle in Composite Materials on Moisture Absorption and Material Degradation After Hygrothermal Ageing, Journal of Reinforced Plastics and Composites, 74(4), 2006, 406-418.
5. B.C. Ray - Hydrothermal Fatigue on Interface of Glass-Epoxy Laminates, *Journal of Reinforced Plastics and Composites*, 24(10), 2005, 1051-1056
6. Liang Li, ShuYong Zhang, YueHui Chen, MoJun Liu, YiFu Ding, XiaoWen Luo, Zong Pu, WeiFang Zhou, and Shanjun Li - Water Transportation in Epoxy Resin, *Chemistry of Materials*, 17(4), 2005, 839-845.
7. B.C. Ray – Effect of Crosshead Velocity & Subzero Temperature on Mechanical Behavior of Hygrothermally Conditioned FRPs, *Material Science and Engineering A*, 379(1-2), 2004, 39-44.
8. S. Pavlidou, C.D. Papaspyrides - The Effect of Hygrothermal History on Water Sorption and Interlaminar Shear Strength of Glass/Polyester Composites with Different Interfacial Strength, *Composites A*, 34(11), 2003, 1117–1124
9. Katya I. Ivanova, Richard A. Pethrick, Stanley Affrossman - Hygrothermal Aging of Rubber Modified and Mineral Filled Dicyandiamide Cured Digylcidyl Ether of Bisphenol A Epoxy Resin. I. Diffusion Behavior, *Journal of Applied Polymer Science,* 82(14), 2001, 3468-3476.
10. B.C. Ray - Loading Rate Effects on Mechanical Properties of Polymer Composites at Ultra Low Temperatures, Journal of Applied Polymer Science, 100(3), 2006, 2289-2292.

11. B.C. Ray – Adhesion of Glass/Epoxy Composites Influenced by Thermal and Cryogenic Environment, Journal of Applied Polymer Science, 102(2), 2006, 1943-1949.
12. W.Noobut, J.L.Koeing - Interfacial Behavior of Epoxy/E-Glass Fiber Composites under Wet-Dry Cycles by FTIR Micro spectroscopy.
13. Peiyi Wu, H.W. Siesler- Water diffusion into epoxy resin: a 2D correlation ATR-FTIR investigation.
14. Hui-Shen Shen, M.Asce - Hygrothermal Effects on the Nonlinear Bending of Shear Deformable Laminated Plates
15. Sergei G. Kazariana, K.L. Andrew Chana, Veronique Maquetb, Aldo R. Boccaccinic - Characterization of bioactive and resorbable polylactide/Bioglasss composites by FTIR spectroscopic imaging.
16. Mikhail V. Motyakin 1, Shulamith Schlick - ESR imaging and FTIR study of thermally treated poly(acrylonitrile-butadiene-styrene) (ABS) containing a hindered amine stabilizer: Effect of polymer morphology, and butadiene and stabilizer content.
17. Gang Xu, Wenfang Shi, Ming Gong, Fei Yu and Jianping Feng - Curing behavior and toughening performance of epoxy resins containing hyper branched polyester Polymer Advanced Technology 2004; 15: 639–644.
18. Y.C. Lin, Xu Chen - Moisture sorption–desorption–resorption characteristics and its effect on the mechanical behavior of the epoxy system, Polymer 46 (2005) 11994–12003.
19. B.C. Ray - Temperature Effect During Humid Ageing on Interfaces of Glass and Carbon Fibers Reinforced Epoxy Composites, Journal of Colloid and Interface Science, 298(1), 2006, 111–117.
20. B.C. Ray - Freeze-thaw Response of Glass-polyester Composites at Different Loading Rates, *Journal of Reinforced Plastics and Composites*, 24(16), 2005, 1771-1776
21. B.C. Ray, S. Mula, T. Bera, P.K. Ray – Prior Thermal Spikes and Thermal Shocks on Mechanical Behavior of Glass Fiber Epoxy Composites, Journal of Reinforced Plastics and Composites, 25(2), 2006, 197-213